

AD-A211 860

RD 5989-EM-01-FR

(2)

DTIC FILE COPY

Project Title: Numerical Model of Two-Dimensional Beach Change

Principal Investigator: Dr. Hans Hanson

Contractor: The University of Lund
Institute of Science and Technology
Department of Water Resources Engineering
Box 118
S-221 00, Lund
SWEDEN

Contract No: DAJA45-88-C-0015

DTIC
ELECTE
AUG 28 1989
S D CL D

Final Report and Users Manual

DISTRIBUTION STATEMENT A

Approved for public release
Distribution Unlimited

The research reported in this document has been made possible through the support and sponsorship of the U.S. Government through its European Research Office of the U.S. Army. This report is intended only for the internal management use of the Contractor and the U.S. Government.

89 8 28 03T

PREFACE

This report was prepared for the Coastal Engineering Research Center (CERC), U.S. Army Corps of Engineers by Magnus Larson and Hans Hanson, Department of Water Resources Engineering, Institute of Science and Technology, University of Lund, Lund, Sweden under Contract DAJA45-88-C-0015. All of the work was carried out in close cooperation with CERC personnel, especially Dr. Nicholas C. Kraus at the Research Division, CERC.

The work was financed through the U.S. Army Research, Development, and Standardization Group - UK, which is gratefully acknowledged.

Accession For	
NTIS CRA&I	<input checked="" type="checkbox"/>
DTIC TAB	<input type="checkbox"/>
Unannounced	<input type="checkbox"/>
Justification	
By <i>perform 50</i>	
Distribution	
Availability Codes	
Dist	
A-1	



CONTENTS

PREFACE	2
LIST OF FIGURES	4
PART I: INTRODUCTION	5
PART II: BEACH CHANGE MODEL OVERVIEW	8
Wave Module	8
Longshore Current Module	15
Cross-Shore Sediment Transport Module	18
Longshore Sediment Transport Module	24
Bottom Contour Orientation Module	25
Beach Change Module	27
PART III: NUMERICAL SOLUTION OF GOVERNING EQUATIONS	32
Wave Module	32
Longshore Current Module	36
Beach Change Module	37
PART IV: ORGANIZATION OF COMPUTER PROGRAM	40
Computer Program Overview	40
Input Data Requirements	41
File Handling in the Program	42
PART V: SAMPLE CALCULATIONS WITH THE BEACH CHANGE MODEL	44
REFERENCES	48
APPENDIX A	51
APPENDIX B	83

LIST OF FIGURES

Figure 1. Comparison between calculated and measured wave height respectively longshore current distribution using data from Visser (1982)	17
Figure 2. Criterion for predicting cross-shore sand transport direction based on monochromatic laboratory data	19
Figure 3. Criterion for predicting cross-shore sand transport direction applied to field conditions	20
Figure 4. Definition sketch for the principal zones of cross-shore transport	21
Figure 5. Comparison between measured and predicted longshore sand transport rates (after Kraus, Gingerich, and Dean 1989)	24
Figure 6. Definition sketch for determining local bottom contour slope	26
Figure 7. Definition sketch for describing avalanching along the profile	28
Figure 8. Definition sketch of numerical grid for beach change model	32
Figure 9. Flow chart describing the subroutines in the beach change computer program	40
Figure 10. Beach change for the case with constant wave height and sinusoidally varying water level	44
Figure 11. Beach change for the case with constant water level and sinusoidally varying wave height	47

NUMERICAL MODEL OF TWO-DIMENSIONAL BEACH CHANGE

PART I: INTRODUCTION

1. The objective of this report is to present a two-dimensional (or schematized three-dimensional) numerical model of beach change due to breaking of short-period waves. The model development aimed at reproducing changes in macro-scale features of the profile, such as bars and berms, especially in the vicinity of coastal structures. As a first step towards a general numerical model for describing the influence of structures on beaches, the evolution of a beach around an impermeable groin or jetty was simulated.

2. A review was made of the literature on beach change modeling. Beach evolution models can be classified into three broad types as:

a. Contour line models, in which the profile is schematized by contour lines which monotonically increase in depth with distance offshore.

b. Two-dimensional (2D) and three-dimensional (3D) models, in which microscale and mesoscale features of the physical processes (waves, currents, sand transport) are described.

c. Cross-shore transport (profile change) models, which simulate cross-shore processes (beach profile change), but neglect longshore processes.

3. Contour line models. The shoreline change simulation model GENESIS (Hanson 1987) defines the state of the art of 1-line models, but it does not include cross-shore sand transport. The zero-depth contour, i.e., shoreline, is taken as the one line characterizing beach change in this type of model. One-line models have been widely used in engineering studies, and n-line models (which simulate the change in several beach contours) have also been developed to predict long-term (order of years) shoreline change (Perlin and Dean 1983). However, n-line models are expensive to run and have seen only restricted use in engineering applications, probably because they give only slightly more information than the

1-line model, but at greatly increased computational cost. Cross-shore sand transport formulations used in n-line models are also greatly simplified and not well verified.

4. 2D and 3D models. There are various levels of 2D and 3D models, but all solve the equation of mass conservation in two horizontal coordinates. They mainly differ by the sophistication of the wave, current, and sediment/sand transport relationships used, and may either compute through the vertical or use depth-averaged quantities. Although descriptions of several 3D and quasi-3D nearshore change models have appeared in the literature, applications have been limited to highly funded projects or pure research testing, with little verification against data from real beaches. Because these models are computationally intensive, they are mainly applicable to projects of relatively small spatial extent (less than approximately 1000 m in longshore extent) and short time periods (less than approximately 1 month). They also require extensive verification and a high level of expertise when implemented.

5. Cross-shore (profile change) models. Two profile change models are presently available for engineering use. One is the model of Kriebel and Dean (1985) which treats the profile schematically and is limited to simulation of erosional events. The other model was developed by Larson and Kraus (1989). This model describes the formation and growth of bars and, to a lesser extent, berms, and it can thus treat a time sequence of erosion and accretion events.

6. On the basis of the literature review and the objective to develop a rapid 2D-model (or schematized 3D) applicable to projects of both small and large spatial extent, it was decided to construct a 2D grided model which would combine the simplicity and reliability of a shoreline change model with a more sophisticated description of profile change. The longshore transport rate calculation was expanded as compared to a traditional shoreline change model to describe the distribution of longshore sand transport across the surf zone (instead of only a total rate as used in 1-line models). The profile change model is run on shore-normal lines to compute cross-shore sand transport rates. Thus, in contrast to previously developed 2D and 3D models, the present model, named "3DBEACH," for schematized 3-Dimensional BEACH Change model, is not employing a complete 2D wave and current calculations, but locally decouples longshore and cross-shore processes and treat them individually as 1-dimensional.

7. The full model 3DBEACH consists in principal of the following five modules:

- a. Wave propagation and decay module.
- b. Longshore current distribution module.
- c. Longshore transport module.
- d. Cross-shore transport module.
- e. Bottom contour orientation module.
- f. Bottom topography change module.

8. In the following chapters is first an overview given of the different parts of the beach change model. This involves a brief discussion of the theoretical foundation of each module and the assumptions behind the calculations. Next chapter presents the numerical solution scheme and the discretization of the governing equations. An short introduction is then given to the computer program as regards input requirements and program operation. Finally, some sample calculations are shown to illustrate the capabilities of the model.

PART II: BEACH CHANGE MODEL OVERVIEW

9. The numerical model consists of various modules which perform calculations independently but are connected through in- and output of wave and sediment transport characteristics. An approach is used which decouples individual profile lines when determining the wave field, cross-shore transport, and longshore transport. The interaction between profile lines are represented through changes in the bottom contours and conservation of sand. The purpose of decoupling the profiles in the calculations is to decrease computational requirements since a normal simulation comprehends many grid points and long simulation times. Solving the two-dimensional, coupled wave equation in space, even in its simplest form, put severe restrictions on length and time step, especially if steep slopes occur which is the case on the seaward side of a bar.

10. At each time step is the wave height distribution determined along every profile line including the processes of shoaling, refraction, and energy dissipation due to breaking. From the wave height calculations are the cross-shore transport rate determined using transport relationships developed by Larson and Kraus (1989). A rapid scheme for calculating the longshore current (Kraus and Larson 1990) is used which forms the basis for determining the longshore transport together with the wave height calculations (Kraus, Gingerich, and Dean 1989). From the cross-shore and longshore transport rate distribution along each profile line the bottom topography change is calculated from the mass conservation equation.

11. In the following a brief description is given of the main modules of the numerical model, that is, modules for calculation of wave height, longshore current, cross-shore transport rate, longshore transport rate, bottom contour orientation, and bottom topography change.

Wave Module

12. The wave height distribution is calculated along each profile line using linear wave theory. Inside the surf zone, after wave breaking, the breaker decay model by Dally, Dean, and Dalrymple (1984) is used to calculate the wave height distribution. The point of incipient wave breaking is determined from an empirical criterion based on the surf similarity parameter (Battjes 1974) expressed in terms of the deepwater wave steepness

and the local beach slope seaward of the breakpoint evaluated over $1/3$ of the wavelength.

13. An input wave height, wave period, and incident wave angle must be given to the model either at deepwater conditions or at a specific depth corresponding to the gage depth. From this information is the wave conditions calculated at the most seaward point of the grid taking into account shoaling and refraction. Energy dissipation in the viscous layer along the bottom is neglected to save execution time since the effect on the wave height is negligible especially in comparison to the amount of energy dissipation during wave braking in the surf zone.

14. The calculation of the wave height distribution across-shore starts in the most seaward calculation cell and proceeds shoreward cell by cell. The local wave height, wavelength, and wave angle with respect to the bottom contours are determined from Snell's law and the conservation of energy flux. When wave breaking occurs energy dissipation due to increased turbulence in the water column is added in the energy flux equation. The main orientation of the bottom contours along a profile line is determined from a special module described later in this report.

15. The energy dissipation in the surf zone is assumed to be proportional to the excess energy flux over a stable energy flux, which is a function of the water depth (Horikawa and Kuo 1966). Wave properties in the surf zone are calculated using linear wave theory with no shallow water approximations. The wave height calculation is carried out to a water depth which is less than the depth where the surf zone ends in accordance with the definition of the different hydrodynamic regions in the nearshore. The depth at the shoreward end of the surf zone is roughly equal to the seaward limit of the backrush.

16. The wave module allows wave reformation to take place leading to several breakpoints and thus surf zones. Wave reformation occurs if the local wave height becomes lower than the stable wave height, implying no wave energy dissipation. When the energy dissipation ceases, shoaling and refraction will become dominant until wave breaking occur again and dissipation is initiated once more.

17. Generalizing the breaker decay model by Dally, Dean, and Dalrymple (1984) the two-dimensional equation for conservation of energy flux incorporating energy dissipation due to wave breaking may be written

$$\partial(F \cos \theta) / \partial x + \partial(F \sin \theta) / \partial y = \kappa / h (F - F_s) \quad (1)$$

where

F = wave energy flux (Nm/m/sec)

θ = wave angle with respect to the bottom contours

x = cross-shore coordinate positive in the seaward direction (m)

y = alongshore coordinate (m)

κ = wave decay coefficient

h = water depth (m)

F_s = stable wave energy flux (Nm/m/sec)

The wave energy flux is given as

$$F = E C_g \quad (2)$$

where

E = wave energy density (Nm/m²)

C_g = wave group velocity (m/sec)

The wave energy density is written using linear wave theory

$$E = 1/8 \rho g H^2 \quad (3)$$

where

H = wave height (m)

ρ = density of water (kg/m³)

g = acceleration of gravity (m/sec²)

Decoupling of the profile lines, equivalent to assuming that the wave conditions are locally uniform alongshore (or varies slowly) and that the bottom contours are locally straight and parallel (or has a small gradient), implies that Equation 1 may be reduced to

$$d(F \cos \theta) / dx = \kappa / h (F - F_s) \quad (4)$$

18. The wave group velocity is related to the velocity of an individual wave C through a factor n which is a function of the water depth and the wavelength L (or wave period T)

$$C_g = n C \quad (5)$$

where

$$n = 1/2 (1 + (2\pi h/L)/\sinh (2\pi h/L)) \quad (6)$$

The speed of a wave is determined through the dispersion relationship

$$C = C_0 \tanh (2\pi h/L) \quad (7)$$

where

$$C_0 = gT/2\pi \quad (8)$$

C_0 is the wave speed at deepwater conditions. Equation 7 is an implicit equation which has to be solved numerically since C contains a dependence on the wavelength, that is $C = L/T$.

19. The wave decay coefficient controls the rate of energy dissipation whereas the stable energy flux determines the amount of energy dissipation necessary in order for stable conditions to occur once breaking is initiated. In this respect stable wave conditions refers to a state when energy dissipation due to wave breaking ceases and thus waves reform. The stable energy flux may be expressed

$$F_s = E_s C_g \quad (9)$$

where

$$E_s = \text{stable wave energy density (Nm/m}^2\text{)}$$

The stable wave energy flux corresponds to a stable wave height which is a function of the water depth

$$H_s = \Gamma h \quad (10)$$

where

$$\Gamma = \text{stable wave height coefficient}$$

20. Two empirical coefficients enter in the breaker decay model namely κ and Γ . However, the values of these coefficients seem to vary negligibly over a wide range of conditions, both in the laboratory and on natural beaches. Dally, Dean, and Dalrymple (1984) recommended the values of $\kappa = 0.15$ and $\Gamma = 0.40$ to be used as an average for a varying bottom

slope based on laboratory and prototype-scale flume data. Ebersole (1987) evaluated the performance of the breaker decay model using field measurements and found good agreement for engineering applications. He also tested the breaker decay model developed by Svendsen (1984) but found it to be inferior in terms of minimizing the root-mean-square error.

21. Larson and Kraus (1989) used prototype-scale data from Kajima et al. (1983) obtained in a large wave tank to verify the applicability of the breaker decay model for a barred beach profile. The values obtained for the two empirical parameters were much in agreement with values obtained by the aforementioned authors. A significant dependence on beach slope for the parameters was noted but no specific relationship was developed.

22. Kraus and Larson (1989) evaluated the performance of the breaker decay model for waves approaching the beach at an angle with respect to the bottom contours both for laboratory (Visser 1982) and field data (Wu, Thornton, and Guza 1985). In these cases no calibration of the model was carried out with respect to the parameters but $\kappa = 0.15$ and $\Gamma = 0.40$ were used. In all cases did the breaker decay model produce satisfactorily agreement. For the field data a statistical approach was used where wave heights were randomly picked from a Rayleigh distribution for a large number of waves and the correspondingly calculated wave height distributions were averaged to obtain a representative distribution.

23. As waves propagate onshore a flux of momentum (radiation stress) arises which causes displacement of the mean water elevation if changes in this flux occurs due to shoaling or breaking. Outside the surf zone shoaling produces an increase in wave height which causes a corresponding increase in the momentum flux. This flux increase is balanced by lowering of the mean water elevation called set-down (Longuet-Higgins and Stewart 1963). Inside the surf zone, as waves continue to break and decrease in wave height, the momentum flux decreases and an increase in mean water elevation occurs known as set-up.

24. The displacement of the mean water surface (set-up or set-down) may be determined from the momentum equation

$$dS_{xx}/dx = -\rho g(h + \eta) d\eta/dx \quad (11)$$

where

S_{xx} = radiation stress in the direction of the waves (N/m)

η = wave set-up or set-down (m)

The radiation stress is given by linear wave theory for an arbitrary wave angle of incidence

$$S_{xx} = 1/8 \rho g H^2 (n (\cos^2 \theta + 1) - 1/2) \quad (12)$$

25. The energy flux conservation equation (Equation 4), the wave dispersion relationship (Equation 7), and the momentum equation (Equation 11) is not sufficient to specify the wave height distribution across-shore if the waves have an angle of incidence with respect to the bottom contours. In this case an additional equation has to be solved which expresses the conservation of wave number. The wave number conservation equation is written in the general form, not taking into account diffraction

$$\partial(\sin\theta/L)/\partial x - \partial(\cos\theta/L)/\partial y = 0 \quad (13)$$

26. For straight and parallel bottom contours, implying no (or mild) alongshore variation in wave and bottom characteristics, Equation 13 may be simplified to yield

$$d(\sin\theta/L)/dx = 0 \quad (14)$$

If Equation 14 is integrated Snell's law is obtained stating that the quantity $\sin\theta/L$ is a constant across-shore. Equations 4, 7, 11, and 14 allows the wave height distribution to be determined once the boundary conditions have been established.

27. As mentioned previously the wave characteristics, such as wave height, period, and incident angle, must be specified at the seaward end of each profile. The end of the grid should be located seaward of the break point at all times. From the wave properties it is possible to determine analytically the set-down at the most seaward point of the profiles (Longuet-Higgins and Stewart 1962)

$$\eta = \pi H^2 / (4L \sinh(4\pi h/L)) \quad (15)$$

28. Also, a condition for the initiation of breaking is needed indicating when energy dissipation due to breaking starts occurring and the

wave decay coefficient becomes different from zero. Breaking occurs when the ratio between the wave height and the water depth exceeds a certain value which is a function of the surf similarity parameter expressed in terms of the deepwater wave steepness and profile slope prior to breaking

$$\gamma = 1.14 \xi^{0.21} \quad (16)$$

where

γ = breaker ratio ($=H_b/h_b$, where index b denotes breaking conditions)

ξ = surf similarity parameter

The surf similarity parameter is given by

$$\xi = \tan\beta / \sqrt{H_0/L_0} \quad (18)$$

where

β = local beach slope seaward of break point

29. Equation 16 was derived by Larson and Kraus (1989) from data given by Kajima et al. (1983) but very similar relationships were previously reported in Singamsetti and Wind (1980) and Sunamura (1980b). Larson and Kraus (1989) used data from prototype-scale experiments whereas the two latter studies were based on small-scale laboratory experiments. Thus, in Equation 16 scale effects seem to be absent although it should be observed that only monochromatic waves were used in the tests with probably negligible wave-by-wave interaction.

30. The experimental data by Kajima et al. (1983) encompass cases with a maximum wave period of 12 sec although most of the cases have periods in the range 3-9 sec. The limited data material for longer period waves, often encountered in the field, makes it necessary to use Equation 16 with care. Also, since the relationship was determined mainly from barred profiles exposed to monochromatic waves, the profile slope seaward of the break point was in general steeper than what is found in the field. Thus, Equation 16 tended to underestimate the breaker ratio in the field for gentle slopes (Larson and Kraus 1989).

31. The energy dissipation due to wave breaking is needed in the prediction of the cross-shore sand transport rate. As the wave height decays after breaking turbulent motion is induced in the surf zone. The turbulent kinetic energy is converted into heat through transfer of energy

from larger to smaller eddies. In the macro-scale approach of the beach profile model it is satisfactory to derive energy dissipation from wave height decay without further resolving the internal structure of this process. However, the difference between the production of turbulent kinetic energy and the corresponding dissipation with reference to the time-scale (Roelvink and Stive 1989) is observed as well as the process of energy reordering (Svendsen, Madsen, and Buhr Hansen 1978).

32. The wave energy dissipation D per unit water volume may be expressed as

$$D = 1/h \, d(F \cos \theta)/dx \quad (19)$$

Using Equation 4 the following relationship for D is obtained

$$D = \kappa/h^2 (F - F_s) \quad (20)$$

Once the wave height distribution is calculated, the energy dissipation per unit water volume is determined explicitly from Equation 20 in the surf zone. Outside the surf zone κ is regarded to be zero and no energy dissipation takes place since bottom friction is neglected.

Longshore Current Module

33. When the wave height distribution has been determined from the wave module the longshore current distribution along each profile line is calculated. A simplified approach involving a rapid numerical solution scheme presented by Kraus and Larson (1990) is used. The governing equation is the momentum equation in the longshore direction (the momentum equation in the cross-shore direction is already used in the wave module to compute the set-up) which is a balance between the change in the alongshore radiation stress directed onshore, the bottom friction, and the lateral mixing due to turbulent diffusion.

34. The governing equation may be written

$$A \, d^2v/dx^2 + dA/dx \, dv/dx - Bv = 1/\rho \, dS_{xy}/dx \quad (21)$$

where

v = longshore current velocity (m/sec)

S_{xy} = alongshore radiation stress directed onshore (N/m)
 The coefficients A and B in Equation 21 is (Kraus and Larson 1990)

$$A = \epsilon (h + \eta) \quad (22)$$

$$B = -2/\pi c_f u_m (1 + \sin^2 \theta) \quad (23)$$

where

ϵ = lateral mixing coefficient (m^2/sec)

c_f = bottom friction coefficient

u_m = maximum bottom orbital velocity (m/sec)

35. The lateral mixing coefficient is proportional to the local maximum orbital velocity and the local wave height according to

$$\epsilon = \Lambda u_m H \quad (24)$$

where the proportionality coefficient is denoted as Λ and has a typical value of 1.0. The bottom friction coefficient normally has a value of about 0.01 for a sandy beach.

36. The alongshore radiation stress directed onshore decreases in the surf zone as the wave height decreases due to breaking and provides the main driving force for the longshore current. This stress is expressed as

$$S_{xy} = 1/16 \rho g H^2 n \sin 2\theta \quad (25)$$

The lateral mixing term in Equation 21 flattens the longshore current distribution and produces a velocity outside the break point where no change in radiation stress occurs.

37. The longshore current module were extensively tested both against laboratory and field data to estimate coefficient values, and to verify the predictive capabilities of the module. The same data sets as were used for the verification of the wave module were applied (Visser 1982, Wu, Thornton, and Guza 1985) together with data from Kraus and Sasaki (1979) and Ebersole and Dalrymple (1980). Ebersole and Dalrymple (1980) presented a hypothetical calculation example for a barred beach which provided a test for the current module regarding numerical stability for a complex bottom

topography and also a possibility to compare with a more sophisticated model of nearshore circulation.

38. The rapid and simplified longshore module used in the beach change model proved to reproduce both the laboratory and field data in a satisfactory manner. Figure 1 displays a comparison between the calculated longshore current distribution and the current distribution measured by Visser (1982) in one of his experiments (case 2). Also, the calculated and measured wave height distribution is shown. The parameter values in the breaker decay model recommended by Dally, Dean, and Dalrymple (1984) were used without any calibration.

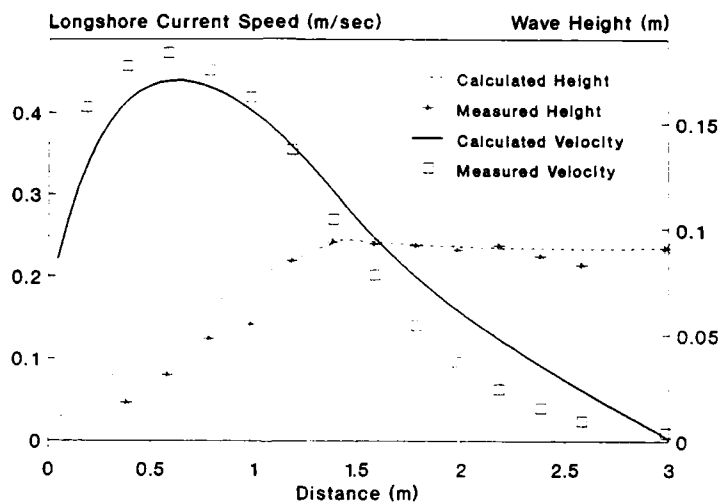


Figure 1. Comparison between calculated and measured wave height respectively longshore current distribution using data from Visser (1982)

39. For the field data, two different techniques were employed to determine the longshore current distribution. In the first case a representative wave height, the root-mean-square wave height, was used in the calculations. In the other case a large number of wave heights were randomly picked from a Rayleigh distribution and the current distribution corresponding to each wave height was determined. To obtain a representative current distribution, the average of all calculated distributions were taken. In comparison with the field data a somewhat better agreement was obtained with the first method if the breaker ratio was put to 0.4.

However, this value is to be regarded as a statistical description of the conditions at an inferred break point, which encompasses both broken and unbroken waves.

40. Accordingly, the second technique was preferred in the simulations since it clearly distinguish between broken and unbroken waves which is of fundamental importance when determining the sediment transport rate. The simulations showed that random forcing conditions in the field could be reproduced by superimposing the effect of a number of monochromatic waves. For the case with a complex bottom topography (Ebersole and Dalrymple 1980) the model proved to be inherently stable and show satisfactory qualitative agreement with the complete circulation model.

Cross-Shore Sediment Transport Module

41. The cross-shore movement of sediment in a surf zone is governed by the properties of the velocity field and the sediment concentration. Thus, a description of the velocity and concentration field is necessary not only across the surf zone but also through the water column at every point. At our present stage of knowledge, such a detailed prediction is not possible in engineering numerical models of beach change to be used on natural beaches. The sediment concentration in the surf zone is closely related to the generation of turbulent motion, which depends on the wave breaking. Accordingly, it is plausible that the sediment concentration, and thus the amount of material available for transport, is closely related to the wave energy dissipation due to wave breaking.

42. In the cross-shore sand transport module, no prediction of the cross-shore velocity field is made but a simple engineering approach is used to determine the transport rate distribution. The direction of the transport is predicted from an empirical criterion derived from the large wave tank data and verified with field data, whereas the magnitude of transport is given by the wave energy dissipation per unit water volume. This simplifying approach implies a transport rate distribution directed either on- or offshore along the entire profile at a specific instant in time.

43. Criterion for predicting the transport direction or the overall profile evolution has been suggested by a number of authors (for a brief review, see Larson and Kraus 1989). This type of criterion normally

comprehends one parameter characterizing the incident wave conditions and one parameter involving some property of the sediments (grain size, D , or fall speed, w). In the present work, the criterion developed by Larson and Kraus (1989) was used involving the two parameters H_o/L_o and H_o/wT (subscript o denotes deepwater conditions), which produced a good distinction between profiles exhibiting on- and offshore sand movement, both in the laboratory and in the field.

44. In Figure 2 is the criterion by Larson and Kraus (1989) displayed (the solid line) together with data from large wave tank experiments. A satisfactory division is achieved described by the equation

$$H_o/L_o = M (H_o/wT)^3 \quad (26)$$

where

H = wave height (m)

L = wavelength (m)

w = sand fall speed (m/sec)

T = wave period (sec)

in which $M = 0.0070$ and the subscript o refers to deepwater conditions. If the left side of Equation 26 is less (greater) than the right side, the profile is predicted to erode (accrete).

45. In the wave tank studies the choice of wave and sediment properties to be used in Equation 26 is trivial due to constant wave forcing conditions and well-defined sediment. However, in order to apply the equation to a natural beach the suitable wave and sediment characteristics have to be found. Field data was therefore collected from various investigations around the world to establish the proper statistical descriptors to be used in Equation 26. The data used are summarized in Sunamura (1980a) and Seymour (1986), where the movement of the deeper contours were used to evaluate profile change and transport direction in the latter investigation.

46. Several different statistical wave characteristics (mean wave height H , root-mean-square wave height H_{rms} , significant wave height H_{so}) were used in order to obtain the best division between on- and offshore (accretion/erosion) sand movement. The mean wave height proved to give the best delineation using the same coefficient values as for the large wave tank data, that is, the wave height in Equation 26 should be taken as the

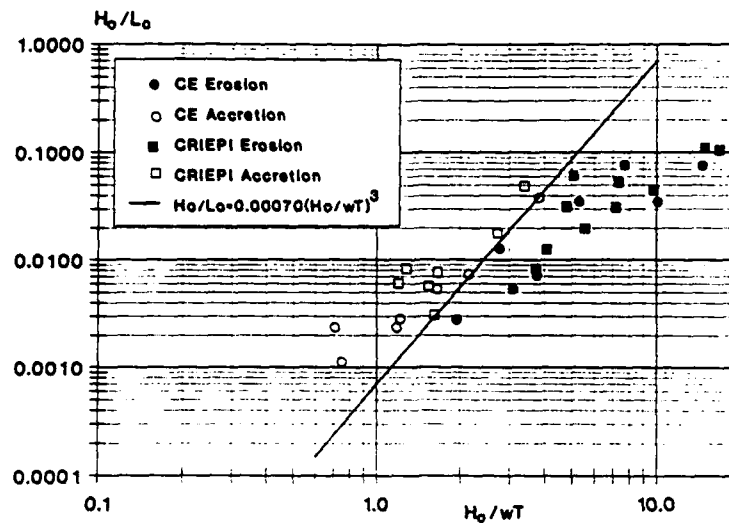


Figure 2. Criterion for predicting cross-shore sand transport direction based on monochromatic laboratory data

mean for field application. Figure 3 displays in analogy to Figure 2 the criterion (solid line) together with the observed data from natural beaches. In the case significant wave height was given, the mean wave height was calculated as $\bar{H} = 0.626 H_{S0}$ from assuming a Rayleigh distribution to be valid for the wave height. The mean or peak period of the spectra was chosen as the representative period to be used in Equation 26 together with the median grain size of the beach sediment.

47. Based on the division of the profile applied in nearshore wave dynamics and the physical characteristics of sediment transport under various flow conditions, four different zones of cross-shore transport along a beach profile were introduced by Larson and Kraus (1989). These zones are

- Zone I: From the seaward depth of effective sand transport to the break point (pre-breaking zone)
- Zone II: From the break point to the plunge point (breaker transition zone)
- Zone III: From the plunge point to the point of wave reformation or to the swash zone (broken wave zone)

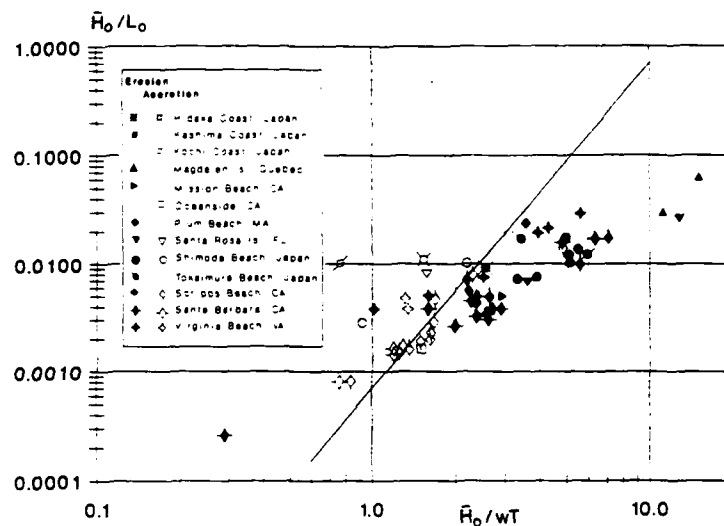


Figure 3. Criterion for predicting cross-shore sand transport direction applied to field conditions

Zone IV: From the shoreward boundary of the surf zone to the shoreward limit of runoff (swash zone)

Figure 4 gives a definition sketch of the different transport zones.

48. The zone between the break point and the plunge point is analogous to the outer region (vortex region according to Miller 1976) proposed by Svendsen, Madsen, and Buhr Hansen (1978). A certain distance is required after breaking before the turbulent conditions are approximately uniform throughout the water column. From a cross-shore transport point of view, assuming the transport rate being proportional to the energy dissipation per unit water volume, the recognition of this zone is important and physically motivated. A more detailed discussion of the different transport zones are given in Larson and Kraus (1989). In this report only the empirically-based transport relationships for the zones derived from the large wave tank data will be presented. These formulas are used in the numerical model to determine the transport rate distribution across-shore.

49. The transport rate relationships derived based on physical considerations and analysis of the large wave tank data may be summarized for the four different zones

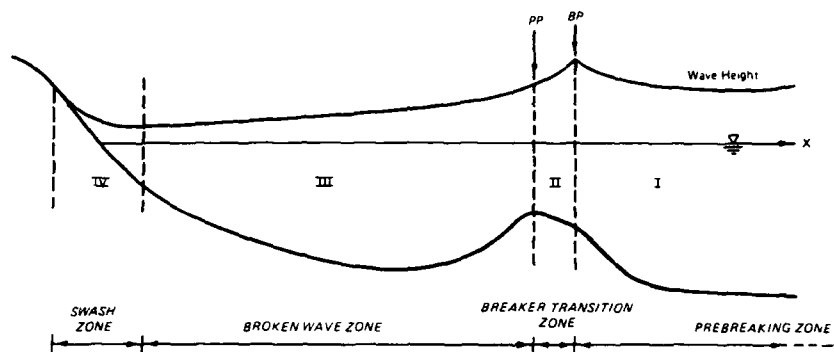


Figure 4. Definition sketch for the principal zones of cross-shore transport

$$\text{Zone I: } q_x = q_b e^{-\lambda_1(x-x_b)} \quad x_b < x \quad (27)$$

$$\text{Zone II: } q_x = q_p e^{-\lambda_2(x-x_p)} \quad x_p < x \leq x_b \quad (28)$$

$$\text{Zone III: } q_x = \begin{cases} K (D - D_{eq} + \epsilon/K dh/dx) & D > D_{eq} - \epsilon/K dh/dx \\ 0 & D < D_{eq} - \epsilon/K dh/dx \end{cases} \quad x_s \leq x \leq x_p \quad (29)$$

$$\text{Zone IV: } q_x = q_s (x - x_r)/(x_s - x_r) \quad x_r < x < x_s \quad (30)$$

where

q_x = cross-shore net transport rate ($m^3/m/sec$)

x = cross-shore coordinate pointing offshore (m)

λ = spatial decay coefficient ($1/m$)

K = transport rate coefficient (m^4/N)

D = wave energy dissipation per unit water volume ($Nm/m^3/sec$)

D_{eq} = equilibrium wave energy dissipation per unit water volume ($Nm/m^3/sec$)

ϵ = slope-related transport rate coefficient (m^2/sec)

h = water depth (m)

The subscripts b, p, s, and r stands (in order) for quantities evaluated at the break point, plunge point, end of the surf zone, and runup limit. Two different spatial decay coefficients are used in Zone I and II (with the subscripts 1 and 2 respectively) to describe the decrease in transport rate with distance.

50. Empirical expression for the spatial decay coefficients were derived from large wave tank data (Larson and Kraus 1989). The decay coefficient in Zone I was related to the median grain size and the breaking wave height

$$\lambda_1 = 10.4 (D_{50}/H_b)^{0.47} \quad (31)$$

In Zone II limited data suggested that

$$\lambda_2 = 0.2 \lambda_1 \quad (32)$$

When calculating the transport rate in Zone I and II the transport rate is first determined at the plunge point from Equation 29 and then the exponential decays are applied seaward in respective zone.

51. The cross-shore transport rate in zones of fully broken waves is related to the wave energy dissipation per unit water volume. This type of transport formula has previously been used by Moore (1982), Kriebel (1982, 1986), and Kriebel and Dean (1985). Analysis of large wave tank data substantiated this type of transport relationship in zones of broken waves (Larson 1988, Larson and Kraus 1989). The transport relationships in the other zones are empirical and based on a large amount of data from wave tank experiments. For example, in the swash zone the transport rate simply decreases linearly from the end of the surf zone to the runup limit. This property of the transport rate distribution appeared for many large wave tank cases, both with on- and offshore sand movement, and similar characteristics have been noted on natural beaches where the beach face receded uniformly during erosional and accretionary events (Seymour 1987).

Longshore Sediment Transport Module

52. Based on the wave height and longshore current calculations the longshore sand transport is determined using the transport formula suggested by Kraus, Gingerich, and Dean (1989). This formula was developed from measurements carried out during two major field experiments at Duck, North Carolina. The transport rate is proportional to the local wave height and longshore current velocity

$$q_y = k (VH - C_c) \quad (33)$$

where k and C_c are empirically determined coefficients. In Figure 5 is a comparison shown from Kraus, Gingerich, and Dean (1989) of transport rates measured in the field and Equation 33, where the wave height was taken as the root-mean-square height.

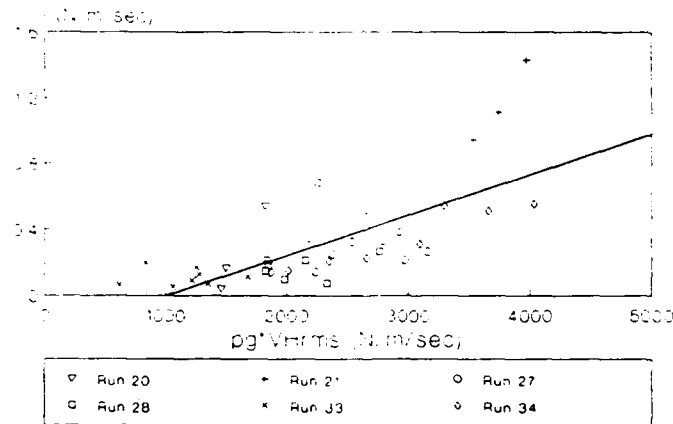


Figure 5. Comparison between measured and predicted longshore sand transport rates (after Kraus, Gingerich, and Dean 1989)

53. Kraus, Gingerich, and Dean (1989) also proposed more complex equations for the longshore transport rate incorporating the spatial derivative of the wave height and the standard deviation of the current velocity. The latter quantity is not possible to estimate but has to be

measured in the field, and thus can not be used in a predictive model. The term containing dH/dx was included initially but omitted later since it became dominant around the break point where the energy dissipation is large.

54. The longshore transport module was extensively tested for various hypothetical wave and water level conditions together with the wave and longshore current module. A maximum in transport rate normally occurs somewhat shoreward of the breakpoint where the product of the local wave height and longshore current has its maximum. Thus, if monochromatic waves and a constant water level are employed, and beach change updrift an impermeable, infinitely long groin (or jetty) is studied, the impoundment will be largest close to the break point. As time elapse a bar-like formation will build up at the groin which eventually prevents the waves from propagating towards the shoreline.

55. If cross-shore sand transport is taken into account this build-up could be reduced as material is transported offshore depending on the relation between the magnitude of longshore and cross-shore transport. In general, however, strong impoundment at the groin around the break point is to be expected due to the distribution of the longshore sediment transport. This build-up normally does not occur in the field but is to be attributed to constant forcing conditions, and the problem is circumvented by introducing some variability in the wave or water level conditions.

56. The longshore sand transport is assumed to occur along the average contour of a specific profile line. This implies that the longshore transport has a component directed in the cross-shore direction when reference is made to the global rectangular coordinate system. Thus, in the beach change model is a calculated longshore transport decomposed with respect to the average bottom contour giving rise to a contribution to the cross-shore transport.

Bottom Contour Orientation Module

57. The bottom contour orientation is important in the calculation of the wave height distribution along each profile line. The incident angle between the wave crests and the bottom contours determines wave refraction and also enters in the wave energy conservation equation. Furthermore, since the contour orientation is dependent upon the local

depth conditions at several neighboring profile lines, the contour scheme introduces a coupling between the beach evolution along the calculation grid.

58. The contouring scheme in the numerical model uses a linear plane to approximate the depth surface around the grid point where the local slope of the contour is to be estimated. From the linear plane equation is the contour slope readily calculated and the average slope given by two planes is used to obtain a slope estimate at the correct grid point location for the wave height calculations. The general equation for a linear plane, used to locally approximate the bottom topography, is

$$h(x,y) = A + Bx + Cy \quad (34)$$

where A, B, and C are coefficients given by the depths in three neighboring grid points. The local slope is then given by

$$dy/dx = -B/C \quad (35)$$

The ratio between the coefficients in Equation 35 may be expressed in terms of grid point depths and distances as

$$B/C = (\Delta y (h_2 - h_1)) / (\Delta x (2h_3 - h_1 - h_2)) \quad (36)$$

where

Δx = cross-shore length step

Δy = longshore length step

A definition sketch explaining the location of the depths used in Equation 36 is given in Figure 6.

59. The slope estimate given by Equation 36 is taken somewhat to the right of the actual grid point location used in the wave height calculation (see Part III). To avoid this another slope-estimate is derived from a linear plane placed through a different set of grid point depths yielding a left-adjusted slope approximation (see Figure 6). The average between the two slope-estimates provides a value at the desired location.

60. The average contour orientation is computed based on the local slope at each grid point for every profile line and used in the wave height calculations. Initially, the local slope at the grid point was used but

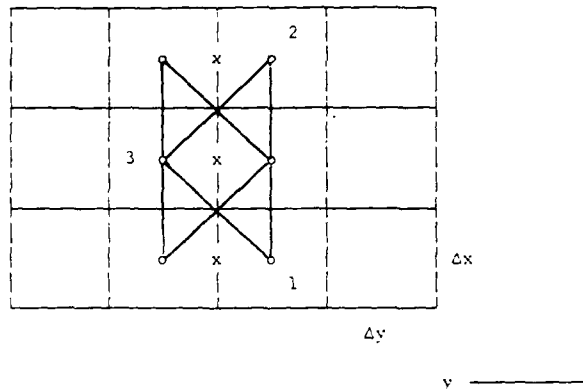


Figure 6. Definition sketch for determining local bottom contour slope

this approach caused difficulties at some grid points for profile lines updrift a groin where strong accretion occurred. Instead the average contour orientation was employed which proved to introduce more stability in the calculations. The use of an average slope implies that the waves respond to the general characteristics of the bottom topography not to local changes in beach bathymetry, which is in agreement with the overall modeling approach.

Beach Change Module

61. The change in bottom topography is calculated from the mass conservation equation, which is written

$$\partial h / \partial t = \partial q_x / \partial x + \partial q_y / \partial y \quad (37)$$

Thus, once the cross-shore and longshore transport rate distribution have been determined, the corresponding beach change is given by Equation 37. Through the sand conservation equation is also the interaction between neighboring profile lines introduced.

62. To avoid excess steepening of profile slopes during conditions when bar growth is significant, under near steady wave and water level forcing, avalanching is allowed to occur. The concept of avalanching, as

discussed by Allen (1970), was incorporated in the numerical model and a routine was included to account for the transport induced by slope failure. Allen (1970) recognized two different limiting profile slopes, namely angle of initial yield (angle of repose) and residual angle after shearing. If the local slope exceeds the angle of initial yield (ψ_i), material is redistributed along the slope and a new stable slope is attained, known as the residual angle after shearing (ψ_r).

63. Analysis carried out by Larson and Kraus (1989) showed values of the maximum slope, inferred as the angle of initial yield, having a mean value of 28 deg. The average value for the residual angle after shearing was determined to be 22 deg, however, the analysis was difficult to carry out since some profile steepening probably occurred between the avalanching and the nearest profile survey in time. Allen (1970) determined from experiments the difference between ψ_i and ψ_r (dilatation angle) to be in the range 10-15 deg for sand. Therefore, in the beach change model is ψ_i set to 28 deg and ψ_r set to 18 deg, that is, a dilatation angle of 10 deg is used.

64. If the local slope exceeds ψ_i the material will be redistributed in the neighboring cells so that the slope everywhere is less or equal ψ_r . Computationally this is carried out by checking the local slope ψ at each time step along the entire grid and if $\psi > \psi_i$ avalanching is initiated. Two conditions determine the redistribution of material, (1) mass should be conserved, and (2) the residual angle after shearing is ψ_r . In Figure 7 a definition sketch is given where the local slope between cell 1 and 2 exceeds ψ_i . Depths before avalanching is denoted with h , whereas the new depths after sand has been redistributed is indicated with a prime.

65. The number of cells N over which the avalanching is occurring is not given a priori but has to be found iteratively. Initially, it is assumed that the avalanching takes place between cell 1 and 2 only. Material is moved from cell 1 to 2 in order to obtain the slope ψ_r between the cells and the new slope between cell 2 and 3 is checked if it exceeds ψ_i . If this is the case, the calculations has to be redone, now incorporating cell 1-3, using the mass conservation equation and assigning the slope ψ_r to all slopes between cells. This procedure is carried out until the slope between cell N and $N+1$ is less than ψ_r .

66. For the general case where sand is to redistributed in N calculation cells included in the avalanching, the mass conservation

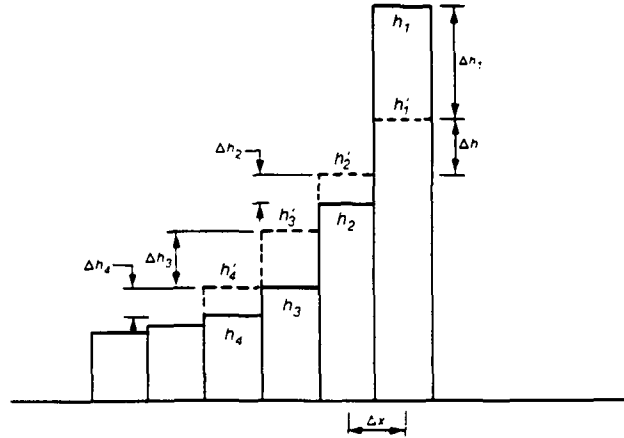


Figure 7. Definition sketch for describing avalanching along the profile
equation is written

$$\sum_{i=1}^N \Delta h_i = 0 \quad (38)$$

where

$$\Delta h_i = h'_i - h_i \quad (39)$$

Observe that the cell numbering, denoted by i , starts from the cell where avalanching is initiated and is taken in the direction of sand redistribution. Also, the depth changes have to be taken with sign. The other criterion necessary to yield the solution is that after avalanching the slope between calculation cells has to be ψ_r . If the length of the calculation cell is Δx , then the residual angle after shearing maybe expressed as

$$\psi_r = (h_i - h_{i+1})/\Delta x \quad (40)$$

Since ψ_r is a constant, the difference in depth between neighboring cells Δh has to be a constant given by

$$\Delta h = \psi_r \Delta x \quad (41)$$

67. The requirement regarding the difference in depth between cells as given by Equation 41 may be written for $N-1$ pair of cells included in the avalanching

$$\begin{aligned} \Delta h &= (h_1 + \Delta h_1) - (h_2 + \Delta h_2) \\ \Delta h &= (h_2 + \Delta h_2) - (h_3 + \Delta h_3) \\ \Delta h &= (h_i + \Delta h_i) - (h_{i+1} + \Delta h_{i+1}) \\ \Delta h &= (h_{N-1} + \Delta h_{N-1}) - (h_N + \Delta h_N) \end{aligned} \quad (42)$$

This system of equations may be rewritten by consecutively eliminating the first part of the right-hand side of each equation by adding the previous equation. The result is

$$\begin{aligned} \Delta h &= (h_1 + \Delta h_1) - (h_2 + \Delta h_2) \\ 2\Delta h &= (h_1 + \Delta h_1) - (h_3 + \Delta h_3) \\ i\Delta h &= (h_1 + \Delta h_1) - (h_{i+1} + \Delta h_{i+1}) \\ (N-1)\Delta h &= (h_1 + \Delta h_1) - (h_N + \Delta h_N) \end{aligned} \quad (43)$$

68. From Equation 43 the unknown depth changes Δh_i may be solved for in every equation

$$\begin{aligned} \Delta h_2 &= (h_1 + \Delta h_1) - h_2 - \Delta h \\ \Delta h_3 &= (h_1 + \Delta h_1) - h_3 - 2\Delta h \\ \Delta h_{i+1} &= (h_1 + \Delta h_1) - h_{i+1} - i\Delta h \\ \Delta h_N &= (h_1 + \Delta h_1) - h_N - (N-1)\Delta h \end{aligned} \quad (44)$$

From Equation 44 it is possible to compute all the depth changes once the depth change in the first cell is known. To determine the depth change in the first cell the mass conservation equation, Equation 38, is used. The sum of all the changes in depth, taken with sign, has to be zero

$$\sum_{i=1}^N \Delta h_i - \Delta h_1 + \sum_{i=2}^N \Delta h_i = 0 \quad (45)$$

Replacing the summation over the depth changes from cell 2 to N using Equation 44 yields

$$\Delta h_1 + \sum_{i=2}^N (h_1 + \Delta h_1) - \sum_{i=2}^N h_i - \sum_{i=2}^N \Delta h = 0 \quad (46)$$

69. From Equation 46 it is possible to explicitly solve for the depth change in cell 1

$$\Delta h_1 = -(N-1)/N h_1 + (\sum_{i=2}^N h_i)/N + (N-1) \Delta h/2 \quad (47)$$

The depth changes in cell 2 to N is then given by

$$\Delta h_i = h_1 + \Delta h_1 - h_i - (i-1) \Delta h \quad (48)$$

PART III: NUMERICAL SOLUTION OF GOVERNING EQUATIONS

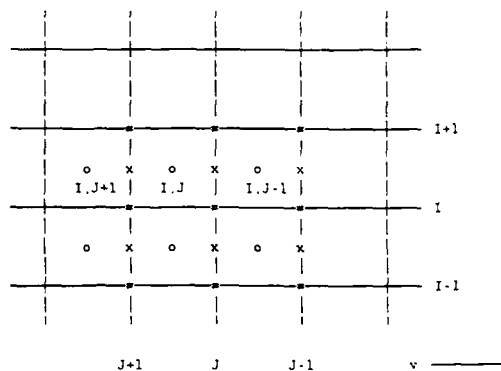
70. In this chapter a brief description is given of the numerical techniques for solving the governing equations in the beach change model. The description is primarily given for the wave module, longshore current module, and beach change module. Also, the boundary conditions in the model are discussed and typical time and length step used in the calculations are presented.

71. In Figure 8 is a definition sketch given of the calculation grid and where the different quantities are taken. The wave height and longshore current computations are carried out in between profile lines using interpolated depths from the original grid (Original depths are denoted as h in Figure 8 whereas interpolated depths between profile lines are named h_{avm} and h_{ave} depending on location in the grid. Note that in the rest of the report, especially in the equations, depth is denoted as h even if it is an interpolated depth for the sake of generality; the context should explain if an interpolated depth is used when calculations are done). Furthermore, before employing the mass conservation equation the cross-shore transport rates has to be interpolated in order to obtain values at the proper grid locations.

72. The index i is used for cross-shore grid point numbering and index j for longshore grid point numbering. The x-axis is positive pointing offshore and the y-axis is directed alongshore according to a right-hand coordinate system with depth h positive below mean sea level.

Wave Module

73. An explicit finite-difference scheme is used to solve the equations for determining the wave height distribution across-shore. In the model a quasi-stationary approach is applied indicating that a time-independent solution of the wave height distribution is determined at every time step. The propagation of individual waves across-shore is not described but it is tacitly assumed that the model time step is significantly larger than the wave period. For irregular wave conditions the wave height used at each time step may be regarded as a statistical measure which represents the average properties of the breaking waves during the time step.



Quantities taken in o-points: h

x-points: δ_b , v , q_y , h_{avm} , u_m , D

#-points: H , δ_w , η , q_x , h_{ave} , F , S_{xx} , S_{xy}

Figure 8. Definition sketch of numerical grid for beach change model

74. The numerical calculation starts at the end of the grid and proceeds onshore for every profile line through an explicit scheme where quantities known at a specific grid point are used to determine corresponding quantities at the next grid point closer to shore. A staggered grid is used with different quantities taken at points in the middle of calculation cells (along a line in between the depths of the original grid) or at the boundaries between cells (see Figure 8). The main quantity in the middle of a cell is the water depth and these grid points will be referred to as x-points (see Figure 8). At the boundaries of calculation cells the main quantity is the cross-shore transport rate and the grid points located here are known as #-points (see Figure 8).

75. From knowing all wave properties at the first grid point (#-point), the wave set-down is determined from Equation 11. The profile depth (h_{avm}) is given in the middle of each calculation cell whereas the set-down (set-up) is calculated at #-points. The depths at the boundaries of the cells (h_{ave}) are given by linear interpolation. Also, the energy flux and the radiation stress in the direction of the waves is determined from knowledge of the depth and wave quantities at the first #-point.

76. When going from a specific #-point to the next, wave refraction is first determined if the incident wave approaches with an angle to the bottom contours. From Equation 14 the angle between the wave crests and the bottom contours at the next #-point onshore is given by

$$\theta_i = \arcsin (L_i/L_{i+1} \sin(\theta_{i+1})) \quad (49)$$

Note that the grid point numbering increases in the seaward direction since the x-axis points offshore, but the calculation proceeds from offshore in the shoreward direction. The water depth at grid point i in Equation 49 is corrected with the set-down (set-up) using the value at grid point $i+1$ in order to avoid an implicit scheme. The wavelengths are calculated using the dispersion relationship (Equation 7) numerically solved by a Pade' approximation (Chen and Thompson 1985).

77. In Equation 49 is θ the angle between the incident wave crests and the bottom contours, whereas the bottom contour orientation with reference to the coordinate system is denoted θ_c and the corresponding wave crest orientation denoted θ_w . Thus, $\theta = \theta_w - \theta_c$ with both angles being positive counterclockwise from the x-axis. As is pointed out in Figure 8, θ_c is taken in a x-point whereas θ_w is calculated in #-points.

78. Next step in the calculation is to determine the energy flux and thus the wave height. Equation 4 is written in difference form

$$F_i = (F_{i+1} (\cos\theta_{i+1} - 0.5A_{ci}) + A_c F_{si})/\cos\theta_i \quad (50)$$

where

$$A_{ci} = \kappa \Delta x / (h_i + \eta_{i+1}) \quad (51)$$

Δx = cross-shore length step (m)

The stable wave energy flux is determined from

$$F_{si} = 1/8 \rho g (\Gamma (h_i + \eta_{i+1}))^2 (C_{gi} + C_{gi+1})/2 \quad (52)$$

An average value for the wave group velocities is used since this quantity is taken at #-points and the stable wave energy flux is evaluated at x-points. Outside the break point, κ should be set to zero, implying that A_{ci} is also zero, since no energy dissipation due to breaking is occurring.

79. When the energy flux has been calculated at a specific point the corresponding wave height is determined from Equations 2 and 3

$$H_i = \sqrt{F_i / (1/8 \rho g C g_i)} \quad (53)$$

Using the wave height, the radiation stress is calculated from Equation 12 and the set-down (set-up) is given from Equation 11 expressed in difference form

$$\eta_i = \eta_{i+1} + (S_{xxi+1} - S_{xxi}) / (\rho g (h_i + \eta_{i+1})) \quad (54)$$

As before η is taken at a #.point half a cell seaward of the x-point when determining the depth to avoid an implicit scheme.

80. At every calculation step a check is made if wave breaking occurs according to the criterion (Equation 16). Once breaking is initiated the wave decay coefficient is given the value $\kappa = 0.15$ and energy dissipation is taking place. Also, if breaking has occurred a check is made if wave reformation is possible, that is, if the wave energy flux is lower than the stable energy flux. The stable wave height coefficient is set to $\Gamma = 0.40$ and if there is wave reformation κ is again given the value zero. An arbitrary number of surf zones with intermediate zones of wave reformation may occur.

81. The wave height calculations are not carried out for the actual profiles but a somewhat smoothed profile is used. The motivation for this is that the response of the wave to the bottom topography takes place over a certain distance suggesting that shoaling and refraction does not occur instantaneously. For instance, on a natural beach a small hump in the bottom would in general not cause a wave to shoal up, which the equations would predict if no profile smoothing was applied. The number of calculation cells over which the smoothing is performed (a moving average scheme) is determined based on the breaking wave height as $3H_b$, where the index b denotes breaking conditions. A simple predictive formula (Larson and Kraus 1989) is used to approximately estimate the breaking wave height at each time step prior to determining the wave height distribution

$$H_b = 0.525 H_o (H_o/L_o)^{-0.25} \quad (55)$$

82. The breaker ratio is determined from Equation 16 for the most seaward break point. If multiple breaking occurs a constant breaker ratio $\gamma = 1.0$ is applied at the consecutive more shoreward break points. The

shoreward boundary of the calculation grid is a predetermined water depth approximately corresponding to the seaward limit of the backrush or the location of a seawall.

Longshore Current Module

83. The longshore current distribution is determined along the same line as where the wave height calculations are carried out. The current velocity is taken at x-points whereas the alongshore radiation stress directed onshore is given at #-points from the wave height computations. A double-sweep solution scheme is employed for solving the tridiagonal system of equations that arises when writing Equation 21 in difference form for all grid points along a profile line. For grid point i the following equation is obtained written in canonical form

$$-AH_i v_{i-1} + BH_i v_i - CH_i v_{i+1} = RH_i \quad (56)$$

where

$$AH_i = -A_i/\Delta x^2 \quad (57)$$

$$BH_i = -(B_i + (A_{i+1} + A_i)/\Delta x^2) \quad (58)$$

$$CH_i = -A_{i+1}/\Delta x^2 \quad (59)$$

$$RH_i = (S_{xyi+1} - S_{xyi})/\Delta x \quad (60)$$

The quantities A and B are defined in Equations 22 and 23, both taken at #-points.

84. By introducing the two double-sweep coefficients E_i and F_i , a recursive equation in the current velocity may be derived

$$v_i = E_i v_{i+1} + F_i \quad (61)$$

By substituting Equation 61, written for index i and i-1, into Equation 60, the following expressions are obtained for the double-sweep coefficients

$$E_i = CH_i/DN_i \quad (62)$$

$$F_i = (AH_i F_{i-1} + RH_i)/DN_i \quad (63)$$

where

$$DN_i = BH_i - AH_i E_{i-1} \quad (64)$$

The solution procedure is thus to determine all E_i and F_i starting from $i=2$ through the whole grid with knowledge about the shoreward boundary condition at grid point $i=1$. The current velocities are then calculated from a backward sweep by using Equation 61 and the seaward boundary condition.

85. The seaward boundary condition is no current velocity at the end of the grid, whereas the shoreward boundary condition is a current velocity corresponding to the explicit solution of Equation 21 neglecting mixing. The current velocity at the most shoreward grid point may be written

$$v_1 = -1/B_1 \, dS_{xy}/dx \quad (65)$$

This is a more realistic description of the current conditions at the shoreline as compared to assuming a zero velocity at the shoreward boundary. From Equations 61 and 65 the values of the double-sweep coefficients at the shoreward boundary is given as $E_1=0$ and $F_1=v_1$. Note that the most shoreward grid point in the longshore current calculation, given the number 1 locally in the current module, corresponds to a higher grid point number in the global calculation grid. The longshore current calculation proceeds shoreward as far as the wave height computation.

Beach Change Module

86. From the calculations carried out in the wave and longshore current module it is possible to determine the cross-shore and longshore transport rate distribution along each profile line. The cross-shore transport rate distributions are given by Equations 27-30 and the longshore transport rate distribution by Equation 33. In this section a brief outline is given of the numerical methods for computing the respective distributions and the discretization of the mass conservation equation.

87. Cross-shore transport distribution. From knowledge of the location of the various transport zones it is possible to calculate the cross-shore transport rate distribution from Equation 27-30. Several break points may occur along a profile if wave reformation takes place leading to

several zones of type II and III. In order to determine the transport rate distribution, the transport rate is first calculated in zones of fully broken waves (Zone III) according to Equation 29 written in difference form

$$q_{xi} = K((D_i + D_{i-1})/2 - D_{eq} + \epsilon/K (h_i - h_{i-1})/\Delta x) \quad (66)$$

The energy dissipation per unit water volume is taken at x-points (in the middle of a calculation cell) making it necessary to average D when calculating the transport rate.

88. The calculation of the transport rate in zones of fully broken waves provides the transport rate at the boundaries of Zone III from which the transport rate may be calculated in the other zones. When the transport rate at the plunge point and at the end of the surf zone is known, Equations 27, 28, and 30 are applied to completely determine the transport rate distribution.

89. Longshore transport rate distribution. From knowledge about the wave height and longshore current distribution the longshore transport rate is calculated using Equation 33 written in difference form

$$q_{yi} = k(v_i(H_{i+1} + H_i)/2 - C_c) \quad (67)$$

The calculated transport rate is regarded as being directed along the average contour orientation of a profile line and decomposed according to the global coordinate system before the mass conservation is employed.

90. Mass conservation equation. The mass conservation equation is solved explicitly to obtain the bottom change at every grid point. The longshore transport rate is given at the same location as the longshore current (see Figure 8) may thus be used directly in the mass conservation equation. Regarding the cross-shore transport rate and the contribution from the longshore transport to the cross-shore transport, interpolation has to be carried out to obtain the transport rate at the proper location. The mass conservation in difference form is expressed as

$$(h_{i,j}^{k+1} - h_{i,j}^k)/\Delta t = (q_{xi+1,j} - q_{xi,j})/\Delta x + (q_{yi,j+1} - q_{yi,j})/\Delta y \quad (68)$$

Δt = time step (sec)

Δy = longshore length step (m)

where the index k denotes a specific time level during which all transport rates are taken.

91. Since the cross-shore transport rate distribution is determined from different relationships depending on the zone of transport, the derivative will in general not be continuous at the boundaries between the zones. To obtain a smoother, more realistic transport distribution a three point filter is applied to the calculated cross-shore transport rates according to

$$q'_{xi} = q_{xi-1}/4 + q_{xi}/2 + q_{xi+1}/4 \quad (69)$$

where the prime denotes the smoothed transport rate. The same type of expression is also applied in the longshore direction to achieve a more gentle variation in q_y , especially in the vicinity of a groin or jetty.

92. The boundary conditions in the beach change calculation differs somewhat in the cross-shore and longshore direction. For each profile line is the cross-shore boundary conditions no sand transport passed certain grid points defined by the length of the active profile. The grid point corresponding to the location of runup constitutes the shoreward boundary, whereas the seaward boundary is determined by how rapid the decay in transport rate seaward of the break point is. When the cross-shore transport rate has decreased to a small predetermined value the calculation is stopped and the current grid point is regarded as the seaward boundary.

93. Two different boundary conditions are possible to specify in the longshore direction, to be discussed more in Part IV. The transport rate may be assumed to be zero at a boundary, corresponding to an impermeable groin, or the boundary may be regarded as an open coast with unaffected transport, that is, no beach change at the boundary due to longshore transport (pinned beach). A typical time step in the model is 5-20 min, a cross-shore length step of 1-5 m, and a longshore length step of 20-50 m.

PART IV: ORGANIZATION OF COMPUTER PROGRAM

94. This chapter describes the organization of the computer code and how to operate the program. Details are given regarding the input data requirements, the external file handling, and the output produced when running the program. The description of the computer code is aiming at being extensive enough to serve as a users manual for applying the program to beach change simulation. In Appendix A is the complete computer program presented with a large number of comment statements to facilitate the understanding of the various parts of the code. Also, in Appendix B is an example of an input file to the program given.

Computer Program Overview

95. The code is separated into a number of different subroutines performing specific tasks in the beach change calculations. In Figure 9 is an overview given of the subroutines and the interaction between the different routines during the calculations. The main program routine is called 3DBEACH and administrates the in- and output of data. Initially general information necessary for the calculation is read in, to be discussed in detail in the next section, together with the depth matrix. Also, 3DBEACH organizes the entire calculation and calls at every time step the subroutines required for computing the beach change.

96. The depth matrix is read in by the subroutine DEPIN with ten depth values given at every line in the input file, with respective profile line appearing as columns in the matrix. WAVIN obtains the wave and water level information at every time step by reading wave height, incident wave angle, wave period, and water level with reference to mean sea level (water level positive above mean sea level). The input wave conditions refer to deepwater conditions or a specific depth.

97. The wave height distribution for every profile line is determined in WAVEHD, which uses the service routine LINWAV to calculate wave properties at a specific depth. CONPLA is also called by WAVEHD in order to determine the bottom contour orientation. After the wave height computations have been carried the longshore current distribution is determined through the routine VELOC. The cross-shore and longshore transport rate distribution is calculated in TRANX respectively TRANY.

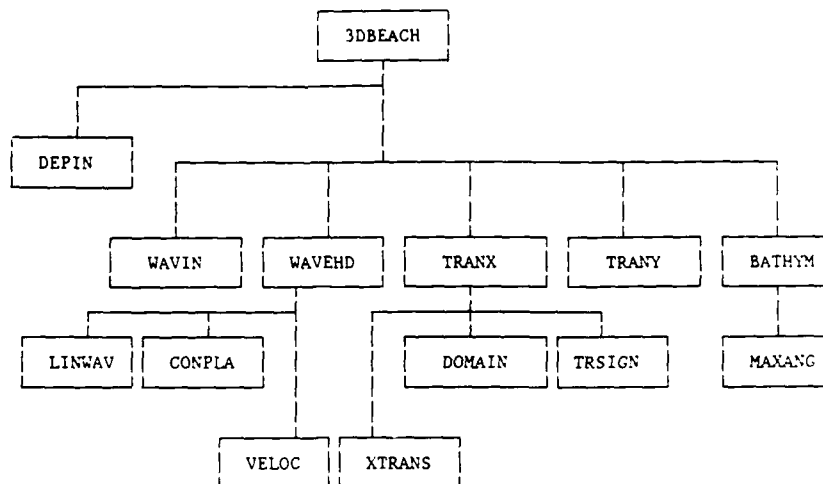


Figure 9. Flow chart describing the subroutines in the beach change computer program

TRANX uses the subroutines DOMAIN to determine the locations of the different cross-shore transport regions, TRSIGN to decide the direction of transport, and XTRANS to calculate the transport rates at every grid point. In BATHYM is the change in bottom topography obtained and by calling the routine MAXANG is a check performed throughout the grid if the angle of repose is exceeded.

Input Data Requirements

98. Besides the depth matrix and wave and water level information at every time step, as previously discussed, some general computational data have to be supplied to run the program. This data should be entered into a start file (file handling is discussed in the next section) which is read by the program before any calculations are performed. In the start file a comment line describing the input separates every line of input data. Appendix B shows the typical structure of an input file containing the necessary computational information.

99. At the top of the input file are four lines of heading which is skipped by the program when reading input data. The first line of input allows a description of the current simulation to be printed out encompassing up to 70 characters. Next line involves the number of time steps, number of grid points in the cross-shore direction, and number of grid

points in the longshore direction. Thereafter should the time step and length step in respective coordinate direction be given. The coefficients required for the longshore current computations must be supplied, that is, the bottom friction coefficient and the mixing parameter.

100. The median grain size of the beach is entered at the next line in units of mm. The output interval, expressed in terms of calculation loops, determines when output information, such as bottom topography and transport rates, is written to different files. A depth has to be supplied where the offshore wave data were collected or if deepwater conditions prevail a negative number should be given on this line. On the next line the coefficients appearing in the longshore respective cross-shore sand transport relationship is entered. The final line in the start file refers to the longshore boundary conditions at the first and last profile line of the grid. The number 0 corresponds to an open coast whereas the number 1 implies an impermeable infinitely long groin or jetty, blocking all sand transport.

101. For some coefficients input values are hardwired in the computer program or given in data statements. In general, these are coefficients with values that are not expected to change from one simulation to another, but may be assumed to be fairly constant. Examples of such coefficients are the two parameters in the breaker decay model and the exponential decay parameters in the cross-shore transport rate distribution (Larson and Kraus 1989).

File Handling in the Program

102. A number of sequential files with specific names which handles the in- and output of data are needed when operating the program. The different files are assigned logical names through open statements. Three files are needed for the input of data and three files are used for the output from the model. The file names given in this report refer to a VAX computer system but the names could easily be modified for implementation on any other system.

103. The general input governing a specific simulation should be stored on a file called START.DAT. As discussed previously, the input data is entered in free format with commentary lines in between lines with data (see Appendix B). The depth matrix is contained in a file named DEPTH.DAT,

where each profile line corresponds to a column in the matrix and ten values are given per line. Wave and water level conditions are punched in free format in the file WAVES.DAT. Wave height, incident wave angle, wave period, and water level is given at every time step entered in free format at one line per time step.

104. The output from the program consists of bottom topography or transport rates at a chosen time increment throughout the simulation together with the conditions at the last time step. Other information from the program, such as wave height and longshore current distribution, has been prepared for printing to various logical units but is tentatively commented out to reduce the amount of output from a simulation. The bottom topography is written to the file DEPUT.DAT in the same format as the input depth matrix. The cross-shore and longshore transport rate distribution along each profile line are stored in the files TRANX.DAT and TRANY.DAT respectively. This is done in the same format as for the depth files.

PART V: SAMPLE CALCULATIONS WITH THE BEACH CHANGE MODEL

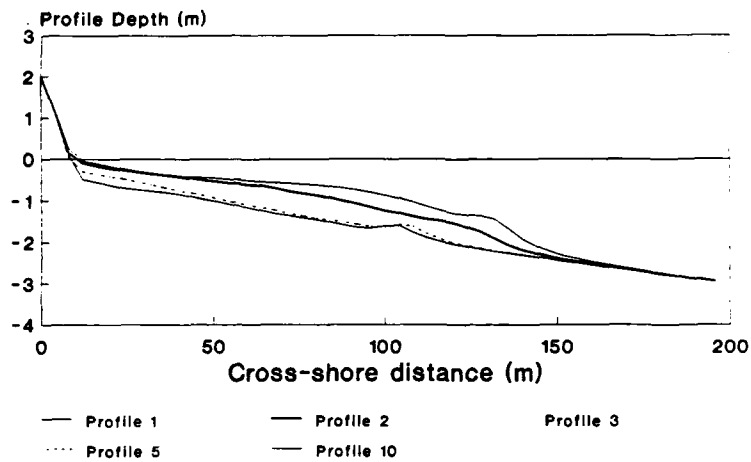
105. In this chapter a number a sample calculations with the beach change model are presented in order to illustrate some of the characteristics of the model. In all cases, the beach evolution updrift a groin was simulated permitting no sand transport past the groin. At the other end of the grid an open coast was assumed (pinned beach) with enough sand supply to prevent any beach change due to longshore transport. Accordingly, cross-shore sand transport may still occur at the profile line located on the boundaries.

106. A spatially distorted grid was used with a length increment of 2 m in the cross-shore direction and 20 m in the longshore direction. The time step was set to 20 min and the total simulation time encompassed 160 time steps. Only a limited grid was used to reduce execution times on the computer namely, 100 grid points across-shore and 10 profile lines along-shore. The initial bottom topography was assumed to be uniform alongshore with a linear dune face and a Dean-type equilibrium profile (Dean 1977) from the shoreline and seaward.

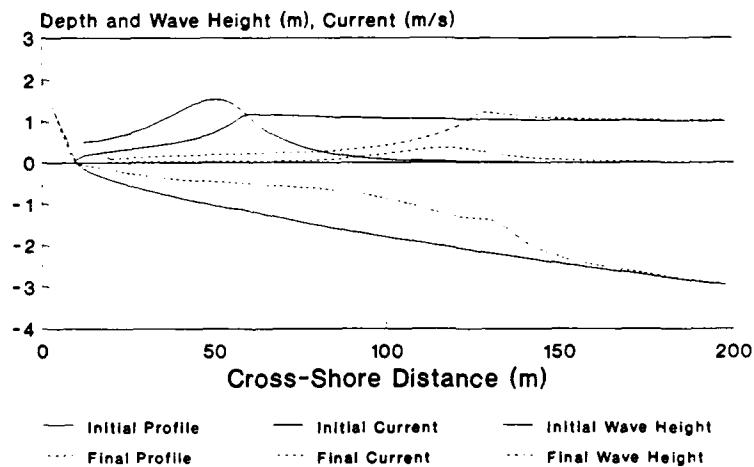
107. Two different wave and water level conditions were studied where the wave height was varied sinusoidally in one case and the water level was varied in the other case. The cycle of variation was 20 time steps for both of the hypothetical simulations. The incident wave angle was set 30 deg in the most seaward calculation cell (end of the grid) and the wave period to 8 sec. In the first case the wave height was constant 1 m and the water level had an amplitude of 0.5 m. For the second case the water level was fixed but the wave height varied between 0.5 and 1.5 m.

108. Figure 10a displays the beach profiles at the last time step for selected profile lines along the grid (profile No. 1, 2, 3, 5, and 10 counting in the direction away from the groin). Significant accumulation occurred along the profile line immediately updrift the groin whereas further away from the groin the accretion was less marked. The steepening of the profile in the seaward part closest to the groin is in qualitative agreement with what is observed in the field. Also, note that the bar feature which is present in the profiles far away from the groin is almost completely obliterated in the profile adjacent to the groin.

109. In Figure 10b is the wave height and longshore current distribution at the initial and final time step for the profile closest to the



(a) beach profiles at final time step for profile lines updrift a groin

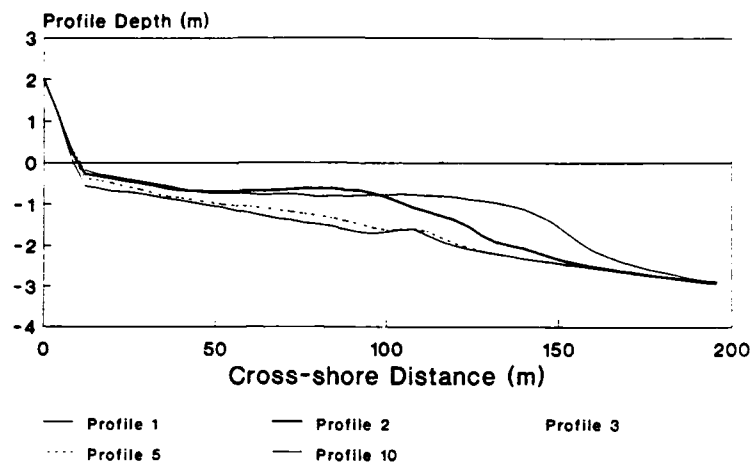


(b) beach profile at initial and final time step and corresponding wave height and longshore current distribution at profile closest to groin

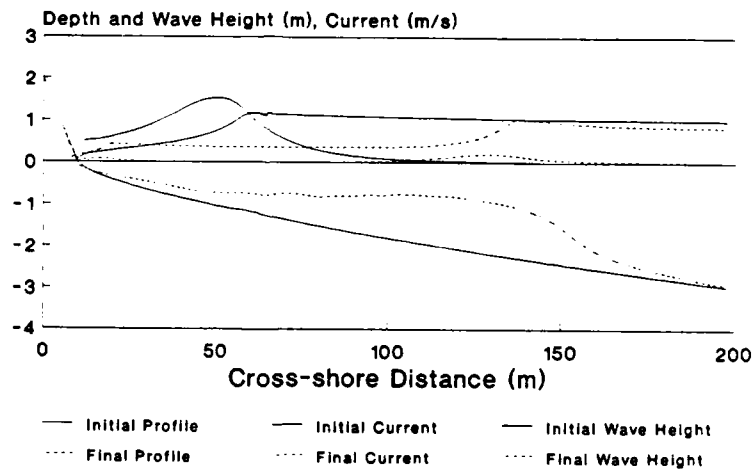
Figure 10. Beach change for the case with constant wave height and sinusoidally varying water level

groin shown. The waves shoal up and break close to shore at the initial profile (the break point located at about 60 m from an arbitrary base line), whereas the break point moves considerably offshore when accumulation takes place (break point at about 125 m). The longshore current distribution is peaked for the initial profile but becomes very flat as material accretes updrift the groin.

110. At Figures 11a and 11b is the corresponding beach evolution displayed for the case of a constant water level and a sinusoidally varying wave height. The beach change is very similar as compared to the case with varying water level although the bar feature is even less noticeable immediately adjacent to the groin. The accumulation updrift the groin is stronger and the seaward movement of the break point is larger. Note that wave reformation takes place at the last time step and two breakpoints occur in Figure 11b.



(a) beach profiles at final time step for profile lines updrift a groin



(b) beach profile at initial and final time step and corresponding wave height and longshore current distribution at profile closest to groin

Figure 11. Beach change for the case with constant water level and sinusoidally varying wave height

REFERENCES

- Allen, J. R. 1970. "The Avalanching of Granular Solids on Dune and Similar Slopes," Journal of Geology, Vol 78, No. 3, pp 326-351.
- Battjes, J. A. 1974. "Surf Similarity," Proceedings of the 14th Coastal Engineering Conference, American Society of Civil Engineers, pp 466-480.
- Chen, H. S., and Thompson, E. F. 1985. "Iterative and Pade' Solutions for the Water-Wave Dispersion Relation," Miscellaneous Paper CERC-85-4, Coastal Engineering Research Center, U.S. Army Engineer Waterways Experiment Station,
- Dean, R. G. 1977. "Equilibrium Beach Profiles: U.S. Atlantic and Gulf Coasts," Department of Civil Engineering, Ocean Engineering Report No. 12, University of Delaware, Newark, DE.
- Dally, W. R., Dean, R. G., and Dalrymple, R. A. 1984. "A Model for Breaker Decay on Beaches," Proceedings of the 19th Coastal Engineering Conference, American Society of Civil Engineers, pp 82-98.
- Ebersole, B. A. 1987. "Measurements and Prediction of Wave Height Decay in the Surf Zone," Proceedings of Coastal Hydrodynamics, American Society of Civil Engineers, pp 1-16.
- Ebersole, B. A. and Dalrymple, R. A. 1981. "Numerical Modeling of Nearshore Circulation," Proceedings of the 17th Coastal Engineering Conference, American Society of Civil Engineers, pp 2710-2725.
- Hanson, H. 1989. "Genesis - a Generalized Shoreline Change Numerical Model," Journal of Coastal Research, Vol 5, No. 1, pp 1-27.
- Horikawa, K., and Kuo, C. 1966. "A Study on Wave Transformation Inside the Surf Zone," Proceedings of the 10th Coastal Engineering Conference, American Society of Civil Engineers, pp 217-233.
- Kajima, R., Saito, S., Shimizu, T., Maruyama, K., Hasegawa, H., and Sakakiyama, T. 1983. "Sand Transport Experiments Performed by Using a Large Water Wave Tank," Data Report No. 4-1, Central Research Institute for Electric Power Industry, Civil Engineering Division, 137 pp. (in Japanese)
- Kraus, N. C. and Larson, M. 1990. "A Numerical Model of Longshore Current," Technical Report CERC-90- , Coastal Engineering Research Center, U.S. Army Engineer Waterways Experiment Station, Vicksburg, Miss. (in preparation)
- Kraus, N. C. and Sasaki, T. O. 1979. "Influence of Wave Angle and Lateral Mixing on the Longshore Current," Marine Science Communications, Vol 5, No. 2, pp 91-126.
- Kraus, N. C., Gingerich, K. J., and Dean, J. 1988. "Toward an Improved Empirical Formula for Longshore Sand Transport," Proceedings of the 21st Coastal Engineering Conference, American Society of Civil Engineers, pp 1182-1196.

Kriebel, D. L. 1982. "Beach and Dune Response to Hurricanes," unpublished M. S. Thesis, University of Delaware, Newark, DE, 334 pp.

_____. 1986. "Verification Study of a Dune Erosion Model," Shore and Beach, Vol 54, No. 3, pp 13-21.

Kriebel, D. L., and Dean, R. G. 1985. "Numerical Simulation of Time-Dependent Beach and Dune Erosion," Coastal Engineering, 9, pp 221-245.

Larson, M. 1988. "Quantification of Beach Profile Change," Report No. 1008, Department of Water Resources Engineering, University of Lund, Lund, Sweden.

Larson, M., and Kraus, N. C. 1989. "SBEACH: Numerical Model for Simulating Storm-Induced Beach Change. Report 1: Empirical Foundation and Model Development," Technical Report CERC-89- , Coastal Engineering Research Center, U.S. Army Engineer Waterways Experiment Station, Vicksburg, Miss. (in press)

Longuet-Higgins, M. S., and Stewart, R. W. 1962. "Radiation Stress and Mass Transport in Gravity Waves with Application to 'Surf Beats'," Journal of Fluid Mechanics, Vol 13, pp 481-504.

_____. 1963. "A Note on Wave Set-up," Journal of Marine Research, Vol 21, pp 4-10.

Moore, B. D., 1982. "Beach Profile Evolution in Response to Changes in Water Level and Wave Height," unpublished M. S. thesis, University of Delaware, Newark, DE, 163 pp.

Perlin, M. and Dean, R. G. 1983. "A Numerical Model to Simulate Sediment Transport in the Vicinity of Coastal Structures," Miscellaneous Report CERC-83-10, U.S. Army Engineer Waterways Experiment Station, Coastal Engineering Research Center.

Roelvink, J. A., and Stive, M. J. F. 1989. "Bar-Generating Cross-Shore Flow Mechanisms on a Beach," Journal of Geophysical Research, Vol 94, No. C4, pp 4785-4800.

Seymour, R. J. 1986. "Results of Cross-Shore Transport Experiments," Journal of the Waterway, Port, Coastal, and Ocean Engineering, Vol 112, No. 1, pp 168-172.

_____. 1987. "An Assessment of NSTS," Proceedings of Coastal Sediments '87, American Society of Civil Engineers, pp 642-651.

Singamsetti, S. R., and Wind, H. G. 1980. "Breaking Waves. Characteristics of Shoaling and Breaking Periodic Waves Normally Incident to Plane Beaches of Constant Slope," Delft Hydraulics Laboratory, Report M 1371.

Sunamura, T. 1980a. "Parameters for Delimiting Erosion and Accretion of Natural Beaches," Annual Report of the Institute of Geoscience, the University of Tsukuba, No. 6, pp 51-54.

_____. 1980b. "A Laboratory Study of Offshore Transport of Sediment and a Model for Eroding Beaches," Proceedings of the 17th Coastal Engineering Conference, American Society of Civil Engineers, pp 1051-1070.

Svendsen, I. A. 1984. "Wave Heights and Set-Up in a Surf Zone," Coastal Engineering, Vol 8, pp 303-329.

Svendsen, I. A., Madsen, P. A., and Buhr Hansen, J. 1978. "Wave Characteristics in the Surf Zone," Proceedings of the 14th Coastal Engineering Conference, American Society of Civil Engineers, pp 520-539.

Visser, P. J. 1982. "The proper longshore current in a wave basin," Report No. 82-1, Department of Civil Engineering, Delft University of Technology.

Wu, C. S., Thornton, E. B., and Guza, R. T. 1985. "Waves and longshore currents: Comparison of a numerical model with field data," Journal of Geophysical Research, Vol 90, No. C3, pp 4951-4958.

APPENDIX A

```

C*****
C* PROGRAM 3DBEACH
C*****
C* IS A 3D-MODEL FOR SIMULATING SHORELINE AND BEACH PROFILE EVOLUTION
C*****
C*
C* PROGRAM EDITORS:
C* HANS HANSON MAGNUS LARSON
C* DEPARTMENT OF WATER RESOURCES ENGINEERING
C* UNIVERSITY OF LUND, SWEDEN
C* AND
C* NICHOLAS C. KRAUS
C* COASTAL ENGINEERING RESEARCH CENTER
C* U.S. ARMY ENGINEER WATERWAYS EXPERIMENT STATION
C* VICKSBURG, MS, USA
C* AUGUST 1988.
C*
C*****
C*
C*** THIS PROGRAM CALCULATES
C***
C*** - THE BREAKING WAVE HEIGHT AND ANGLE
C***
C*** - WAVE HEIGHT DECAY INSIDE BREAKER ZONE
C***
C*** - CROSS-SHORE TRANSPORT RATES QX(Y)
C***
C*** - LONGSHORE CURRENT VELOCITY DISTRIBUTION V(X)
C***
C*** - LONGSHORE TRANSPORT RATE DISTRIBUTION QY(X)
C***
C*** - NEW BOTTOM BATHYMETRY DEP(X,Y) USING QX(Y) AND QY(X)
C***
C*****
C*** INDEX: Z-DEEP WATER, IN=INITIAL, BR=BREAKING
C*** SWL=SEAWALL, GR=GROIN, OB=OFFSHORE BOUNDARY
C***
C*****
C***
C***
C*-----
C* PARAMETER(MM=100,NN=50,NNGR=10,NM=NN*MM,
&M1=MM+1,N1=NN+1,NM1=M1*N1)
C* REAL KX,KY,NY
C* CHARACTER*70 TITLE
C*
C* REAL D(MM,NN),DSMO(MM,NN),E(M1),QXT(M1,N1)
C* REAL H(M1),QX(M1,N1),QY(M1,N1),V(M1),DISS(MM)
C* REAL DIN(MM,NN),CEXO(5),ZC(MM),QYX(M1,N1),DCHG
C* REAL HBEG,ZBEG,T,DHTOT(M1),DH(M1),DMEAN(MM)
C* REAL QSMOX(M1),QSMOY(M1),VPRI(M1),HPRI(M1)
C* INTEGER ISHORE(NN),NBR(M1),IYGR(NNGR)
C* INTEGER IGTIP(NNGR),ISEAWL(NN)

```

```

C*
COMMON /BLOCKA/DX,DY,DTX,M,N,G,PI,GAMMA
COMMON /BLOCKB/D50,SRATIO,NY,SLOPE,DFS
COMMON /BLOCKC/CQ,CEQ,CEXO,EPS
COMMON /BLOCKD/CRED,CEXR,AEXP
COMMON /BLOCKE/HBEG,ZBEG,T,DCHG,CC,DOFF
COMMON /BLOCKF/CF,GAMMIX,KY,QCUT
COMMON /BLOCKG/IBRICH,IBLEFT

C*
C*INITIALIZE
C*
DATA QX/NM1*0./,QY/NM1*0./,V/M1*0./
DATA G/9.806/,PI/3.141593/,GAMMA/1.0/
DATA NY/1.2E-6/,SRATIO/2.65/,SLOPE/0.02/,EPS/2.E-3/
DATA CRED/0.2/,CEXR/0.1/,AEXP/0.5/,DFS/0.5/
DATA QCUT/0.0E-5/CC/1226./

C*
C*FILE PREPARATION & READING
C*
OPEN (UNIT=10,NAME='START.DAT',STATUS='UNKNOWN')
OPEN (UNIT=12,NAME='DEPTH.DAT',STATUS='UNKNOWN')
OPEN (UNIT=16,NAME='WAVES.DAT',STATUS='UNKNOWN')
OPEN (UNIT=18,NAME='TRANX.DAT',STATUS='UNKNOWN')
OPEN (UNIT=20,NAME='TRANX.DAT',STATUS='UNKNOWN')
OPEN (UNIT=22,NAME='DEPUT.DAT',STATUS='UNKNOWN')

C*
C* READ FILE HEADING
C*
DO 8 I=1,4
  READ(10,*)
8  CONTINUE
C*
C* RUN TITLE
C*
  READ(10,*)
  READ(10,503) TITLE

C*
C* NUMBER OF CALCULATION TIME LOOPS & GRID CELLS
C*
  READ(10,*)
  READ(10,*) NCL,M,N

C*
C* ERROR CHECK AND MESSAGE
C*
  IF(N.GT.NN) THEN
    WRITE(*,*) 'ERROR. TOO MANY CALCULATION CELLS IN X-DIRECTION.'
    WRITE(*,*) 'PLEASE CHANGE VALUE OF "N" IN INPUT FILE.'
    NOCON=1
    GOTO 116
  ENDIF
  IF(M.GT.MM) THEN
    WRITE(*,*) 'ERROR. TOO MANY CALCULATION CELLS IN Y-DIRECTION.'
    WRITE(*,*) 'PLEASE CHANGE VALUE OF "M" IN INPUT FILE.'
    NOCON=1
    GOTO 116
  ENDIF
ENDIF

```

```

C*
C* CROSS-SHORE AND LONGSHORE TIME INCREMENT & SPACE INTERVAL
C*
      READ(10,*)
      READ(10,*) DTX,DX,DY
      DTXM=DTX
      DTX=DTX*60.
C*
C* LONGSHORE TRANSPORT PARAMETERS
C*
      READ(10,*)
      READ(10,*) CF,GAMMIX
C*
C* MEDIAN SAND GRAIN SIZE (IN MM)
C*
      READ(10,*)
      READ(10,*) D50
      D50=D50/1000.
C*
C* OUTPUT INTERVAL EXPRESSED AS NO. OF CALCULATION LOOPS
C*
      READ(10,*)
      READ(10,*) IOUT
C*
C* DEPTH CORRESPONDING TO OFFSHORE WAVE DATA
C*
      READ(10,*)
      READ(10,*) DOFF
C*
C* SAND TRANSPORT CALIBRATION COEFFICIENTS (KY=L-S, KX=C-S)
C*
      READ(10,*)
      READ(10,*) KY,KX
      CQ=KX*1.E-6
C*
C* INPUT BOUNDARY CONDITIONS AT RIGHT AND LEFT SIDE OF GRID
C* (0=OPEN COAST, 1=IMPERMEABLE GROIN)
C*
      READ(10,*)
      READ(10,*) IBRIGH,IBLEFT
C*
C* INITIAL SCREEN MESSAGES
C*
      WRITE(*,*) CHAR(12)
      WRITE(*,*) 'C O A S T A L   E N G I N E E R I N G   R E S E A R C
&H   C E N T E R '
      WRITE(*,*)
      WRITE(*,*) ' *****      *****      *****      *****      *****      .**
& **   **   **'
      WRITE(*,*) ' *****      *****      *****      *****      *****      ****
& ***   **   **'
      WRITE(*,*) ' **   **   **   **   **   **   **   **   **   **   **
& **   **   **'
      WRITE(*,*) ' **   **   **   **   **   **   **   **   **   **   **
& **   **   **'

```

```

WRITE(*,*) '      ** ** ** ** ** ** ** ** ** ** **   ** ** **
&  ** **'
WRITE(*,*) '      ** ** ** ***** ***** ***** **
&  *****'
WRITE(*,*) '      ** ** ** ***** ***** ***** **
&  *****'
WRITE(*,*) ' **      ** ** ** ** **   ** ** **
&  ** **'
WRITE(*,*) ' **      ** ** **     ** ** **
& ** ** **'
WRITE(*,*) ' **      ** ** **     ** ** **
& ** ** **'
WRITE(*,*) ' ***** ***** ***** ***** ** ** ****
& *** ** **'
WRITE(*,*) ' ***** ***** ***** ***** ** ** ****
& *** ** **'
WRITE(*,*)
C*
C* CONFIRMATION ON SCREEN
C*
WRITE(*,612) 'RUN: ',TITLE
WRITE(*,*)
WRITE(*,*) ' KX =',KX,'   KY =',KY,'           NCL =',NCL
WRITE(*,*) ' DX =',DX,'   DTX =',DTXM,' MIN'
WRITE(*,*) ' M =',M,'   N =',N
C*
C* READ AND SAVE INITIAL BOTTOM CONFIGURATION
C*
CALL DEPIN(DIN)
DO 29 I=1,M
  DO 30 J=1,N
    D(I,J)=DIN(I,J)
30  CONTINUE
29  CONTINUE
C*
C* CALCULATING EQ. PROFILE SHAPE FACTOR
C*
DD50=DD50*1000.
IF(DD50.LT.0.4) ADEAN=0.41*DD50**.94
IF(DD50.GE.0.4.AND.DD50.LT.10.) ADEAN=0.23*DD50**.32
IF(DD50.GE.10..AND.DD50.LT.40.) ADEAN=0.23*DD50**.28
IF(DD50.GE.40.) ADEAN=0.46*DD50**.11
C*
C* EQUILIBRIUM ENERGY DISSIPATION
C*
CEQ=0.75*ADEAN**1.5*3902.
C*
C*****
C* MAIN CALCULATION LOOP *
C*****
C*
DO 115 NS=1,NCL
  KKK=0
  IF(NS.EQ.1.OR.NS.EQ.NCL) KKK=1

```

```

C*
C* OBTAIN WAVE DATA ALONG THE COAST AT END OF GRID
C*
      CALL WAVIN(D)
C*
C* ADD WATER LEVEL CHANGE
C*
      DO 49 J=1,N
        DO 48 I=1,M
          D(I,J)=D(I,J)+DCHG
48      CONTINUE
49      CONTINUE
C*
C* SMOOTH BOTTOM PROFILE FOR WAVE CALCULATION
C*
      MAV=9
      DO 51 J=1,N
        DO 52 I=M,1,-1
          IF(I.GT.M-MAV/2)THEN
            DSMO(I,J)=D(I,J)
          ELSEIF(I.LE.M-MAV/2.AND.D(I-MAV/2,J).GT.0)THEN
            SUM=0
            DO 53 K=I-MAV/2,I+MAV/2
              SUM=SUM+D(K,J)
53          CONTINUE
            DSMO(I,J)=SUM/REAL(MAV)
          ELSE
            DO 54 K=1,I
              DSMO(K,J)=D(K,J)
54          CONTINUE
            GOTO 51
          ENDIF
68      CONTINUE
51      CONTINUE
C*
C* CALCULATE FOR EACH PROFILE
C*
C*
      DO 87 J=1,N+1
C*
C* DETERMINE MEAN PROFILE
C*
      DO 68 I=1,M
        IF(J.EQ.1)THEN
          DMEAN(I)=D(I,J)
        ELSEIF(J.EQ.N+1)THEN
          DMEAN(I)=D(I,J-1)
        ELSE
          DMEAN(I)=0.5*(D(I,J)+D(I,J-1))
        ENDIF
68      CONTINUE
C*
C* DETERMINE THE WAVE HEIGHT DISTRIBUTION
C*
      CALL WAVEHD(KKK,DSMO,J,H,E,V,DISS,ISTOP,NBR,ZC,
&      ZCM)

```



```

DO 69 I=1,M+1
  IF(I.EQ.1)THEN
    DH(I)=DMEAN(I)
  ELSEIF(I.EQ.M+1)THEN
    DH(I)=DMEAN(M)
  ELSE
    DH(I)=0.5*(DMEAN(I)+DMEAN(I-1))
  ENDIF
  DHTOT(I)=DH(I)+E(I)
69  CONTINUE
C*
C* DETERMINE CROSS-SHORE TRANSPORT
C*
      CALL TRANX(J,H,DISS,NBR,DMEAN,DH,DHTOT,NRU,
&      NFS,QXT)
C*
C* DETERMINE LONGSHORE TRANSPORT
C*
      CALL TRANY(J,ISTOP,NRU,NFS,NBR,V,H,ZC,ZCM,QY,QYX)
C*
C* WRITE WAVE HEIGHT AND LONGSHORE CURRENT AT FIRST AND LAST TIME
C* STEP FOR PLOTTING
C*
      IF(KKK.EQ.1.AND.J.EQ.1)THEN
        NPRI=ISTOP
        DO 383 I=NPRI,M
          VPRI(I)=-V(I)
          HPRI(I)=H(I)
383    CONTINUE
          HPRI(M+1)=H(M+1)
        ENDIF
87    CONTINUE
C*
C* SPECIAL CASE OF OPEN COAST AT RIGHT END OF GRID
C*
      IF(IBRIGH.EQ.0)THEN
        DO 38 I=1,M
          QY(I,1)=QY(I,2)
38    CONTINUE
        ENDIF
C*
C* INTERPOLATE CROSS-SHORE TRANSPORT RATES ALONG DEPTH GRID
C*
      DO 33 J=1,N
        QX(1,J)=0.0
        DO 43 I=2,M
          QAA=0.25*(QYX(I,J)+QYX(I-1,J)+QYX(I,J+1)
&          +QYX(I-1,J+1))
          QX(I,J)=0.5*(QXT(I,J)+QXT(I,J+1))+QAA
43    CONTINUE
          QX(M+1,J)=0.0
33    CONTINUE

```

```

C*
C* CHANGE BACK TO ORIGINAL WATER LEVEL BEFORE APPLYING THE
C* MASS CONSERVATION EQUATION
C*
      DO 57 J=1,N
      DO 58 I=1,M
      D(I,J)=D(I,J)-DCHG
C*
C* SMOOTH TRANSPORT RATES ALONGSHORE AND CROSS-SHORE
C*
      IF(I.GT.1.AND.I.LT.M)THEN
      QSMOX(I)=0.25*QX(I-1,J)+0.50*QX(I,J)+0.25*QX(I+1,J)
      QSMOY(I)=0.25*QY(I-1,J)+0.50*QY(I,J)+0.25*QY(I+1,J)
      ENDIF
58      CONTINUE
      DO 100 I=1,M
      QX(I,J)=QSMOX(I)
      QY(I,J)=QSMOY(I)
100      CONTINUE
57      CONTINUE
C*
C* DETERMINE THE CHANGES IN BATHYMETRI
C*
      CALL BATHYM(QX,QY,D)
      IF(KKK.EQ.1)THEN
      WRITE(50,*) M
      DO 333 I=1,M
      WRITE(50,*) REAL(I-1)*DX,-D(I,1)
333      CONTINUE
      WRITE(50,*) M-NPRI+1
      DO 334 I=NPRI,M
      WRITE(50,*) REAL(I-1)*DX,VPRI(I)
334      CONTINUE
      WRITE(50,*) M-NPRI+1
      DO 335 I=NPRI,M
      WRITE(50,*) REAL(I-1)*DX,0.5*(HPRI(I)+HPRI(I+1))
335      CONTINUE
      DO 336 I=1,M
      WRITE(51,110) -D(I,1),VPRI(I),0.5*(HPRI(I)+HPRI(I+1))
110      FORMAT(' ',3F8.3)
336      CONTINUE
      ENDIF
C*
C* INTERMEDIATE OUTPUT
C*
      IF(MOD(NS,IOUT).EQ.0.OR.NS.EQ.NCL) THEN
C*
C* WRITE L-S TRANSPORT QY, C-S TRANSPORT QX, AND DEPTH
C*
      IMAT=N/10
      IF(IMAT.NE.0) THEN
      IMOD=MOD(N,10)
      II=0
      IIM=-9
      DO 50 IMOUT=1,IMAT
      II=II+10

```

```

IIM=IIM+10
WRITE(18,*) 'QY*10**4 FOR J= ',IIM,' TO ',II,
&      ' FOR TIMESTEP ',NS
WRITE(18,600) ((QY(I,J)*10.**4,J=IIM,II),I=1,M)
WRITE(20,*) 'QX*10**4 FOR J= ',IIM,' TO ',II,
&      ' FOR TIMESTEP ',NS
WRITE(20,600) ((QX(I,J)*10.**4,J=IIM,II),I=1,M)
WRITE(22,*) 'DEPTH FOR J= ',IIM,' TO ',II,
&      ' FOR TIMESTEP ',NS
WRITE(22,600) ((-D(I,J),J=IIM,II),I=1,M)
50 CONTINUE
ENDIF
IF(IMOD.NE.0) THEN
II=II+IMOD
IIM=IIM+10
WRITE(18,*)
WRITE(18,*) 'QY*10**4 FOR J= ',IIM,' TO ',II
WRITE(18,600) ((QY(I,J)*10.**4,J=IIM,II),I=1,M)
WRITE(20,*) 'QX*10**4 FOR J= ',IIM,' TO ',II
WRITE(20,600) ((QX(I,J)*10.**4,J=IIM,II),I=1,M)
WRITE(22,*) 'DEPTH FOR J= ',IIM,' TO ',II
WRITE(22,600) ((-D(I,J),J=IIM,II),I=1,M)
ENDIF
ENDIF
115 CONTINUE
116 IF(NOCON.EQ.1) THEN
WRITE(*,*) 'EXECUTION STOPPED'
ENDIF
C*
C* END-OF-COMPUTATION SIGNAL (BELL)
C*
WRITE(*,*) CHAR(7),CHAR(7)
C*
C* FORMAT STATEMENTS FOR OUTPUT
C*
503 FORMAT(3X,A70)
600 FORMAT(10F7.3)
601 FORMAT(/1X,'OUTPUT LAST TIME STEP NO.',I7/)
602 FORMAT(1X,I017)
603 FORMAT(/1X,'BREAKING WAVE HEIGHT'/(1X,10F7.2))
604 FORMAT(/1X,'BREAKING WAVE ANGLE'/(1X,10F7.1))
605 FORMAT(/1X,'BREAKING WAVE LOCATION'/(1X,I017))
610 FORMAT(10I7)
612 FORMAT(1X,A4,1X,A70)
614 FORMAT(1X,A,I3,A,I3)
616 FORMAT(10F7.2)
END

```

```

C*
C*****
      SUBROUTINE DEPIN(DEP)
C*****
C*
C* READS DEPTHS FROM A FILE
C*
      PARAMETER(MM=100,NN=50,NNGR=10,NM=NN*MM,
&M1=MM+1,N1=NN+1,NM1=M1*N1)
C*
      REAL DEP(MM,NN)
C*
      COMMON /BLOCKA/DX,DY,DTX,M,N,G,PI,GAMMA
C*
C* READ DEPTHS ALONG THE COAST
C*
      IMAT=N/10
      IF(IMAT.NE.0) THEN
        IMOD=MOD(N,10)
        II=0
        IIM=-9
        DO 5 IDEP=1,IMAT
          II=II+10
          IIM=IIM+10
          READ(12,*)
          READ(12,600,END=99) ((DEP(I,J),J=IIM,II),I=1,M)
5          CONTINUE
        ENDIF
        IF(IMOD.NE.0) THEN
          II=II+IMOD
          IIM=IIM+10
          READ(12,*)
          READ(12,600,END=99) ((DEP(I,J),J=IIM,II),I=1,M)
        ENDIF
        GOTO 60
      CONTINUE
99      WRITE(*,*) 'ERROR FOUND IN "DEPIN".'
      WRITE(*,*) 'FILES "DEPTH" (AND "WAVES")'
      WRITE(*,*) 'CONTAIN TOO FEW VALUES.'
      WRITE(*,*) 'PLEASE CHANGE IN DATA FILE(S).'
      NOCON=1
      GOTO 100
60      CONTINUE
C*
600     FORMAT(10F7.2)
100     CONTINUE
      RETURN
      END

```

```

C*
C*****
      SUBROUTINE WAVIN(D)
C*****
C*
C* READS OFF-SHORE WAVE DATA FROM A WAVE FILE
C*
      PARAMETER(MM=100,NN=50,NNGR=10,NM=NN*MM,
&M1=MM+1,N1=NN+1,NM1=M1*N1)
      REAL D(MM,NN),HBEG,ZBEG,DCHG
      COMMON/BLOCKA/DX,DY,DTX,M,N,G,PI,GAMMA
      COMMON/BLOCKE/HBEG,ZBEG,T,DCHG,CC,DOFF
C*
C* READ DEEP WATER WAVE CONDITIONS
C*
66      READ(16,*,END=99,ERR=77) HOFF,ZOFF,T,DCHG
      HBEG=HOFF
      ZBEG=ZOFF
C*
C* REACHED END OF WAVE DATA FILE. REWIND, READ HEADING AND CONTINUE.
C*
      RETURN
99      REWIND 16
      GOTO 66
77      WRITE(*,*) 'ERROR IN WAVIN'
      STOP
      END

```

```

C*
C*****
      SUBROUTINE TRANX(IP,H,DISS,NBR,DMEAN,DH,DHTOT,NRU,NFS,QX)
C*****
C*
C* THIS ROUTINE CALLS THE SUBROUTINES NECESSARY FOR GENERATING
C* THE CROSS-SHORE TRANSPORT RATES FOR A SPECIFIC PROFILE J
C*
      PARAMETER(MM=100,NN=50,NNGR=10,NM=NN*MM,
&M1=MM+1,N1=NN+1,NM1=M1*N1)
      REAL QX(M1,N1),DX,DY,DTX,Q(M1),DMEAN(MM),
&H(M1),DISS(MM),DH(M1),DHTOT(M1)
      INTEGER NBR(M1),NPE(5),NPP(5),NPB(5),SIGN,NRU,NFS
C*
      COMMON /BLOCKA/DX,DY,DTX,M,N,G,PI,GAMMA
C*
C* DETERMINE LOCATIONS OF TRANSPORT REGIONS
C*
      CALL DOMAIN(DH,DHTOT,NBR,H,NRU,NFS,NPE,NPP,NPB,NRBPE)
C*
C* DETERMINE DIRECTION OF TRANSPORT
C*
      CALL TRSIGN(SIGN)
C*
C* DETERMINE CROSS-SHORE TRANSPORT RATES
C*
      CALL XTRANS(SIGN,DMEAN,NRU,NFS,NPE,NPP,NPB,NRBPE,DISS,Q)
      DO 20 I=1,M+1
        QX(I,IP)=Q(I)
20    CONTINUE
      RETURN
      END

```

```

C*
C*****
      SUBROUTINE DOMAIN(DH,DHTOT,NBR,H,NRU,NFS,NPE,NPP,NPB,NRBPE)
C*****
C*
C* THIS ROUTINE DETERMINES THE LOCATION OF THE BOUNDARIES OF
C* THE DIFFERENT CALCULATION DOMAINS.
C*
      INTEGER MM,NN,M,N,I,NFS,NPP(5),NRU,NPE(5),NPB(5)
      PARAMETER(MM=100,NN=50,NNGR=10,NM=NN*MM,
&M1=MM+1,N1=NN+1,NM1=M1*N1)
      INTEGER NBR(M1),J,L,NRBPE
      REAL DHTOT(M1),DFS,LO,T,HO,DX,DY,DTX,EPS,GAMMA,DH(M1),
&H(M1),CQ,CEQ,DRU,SRATIO,D50,CEXO(5),NY,DCHG
      LOGICAL OK1,OK2
C*
      COMMON/BLOCKA/DX,DY,DTX,M,N,G,PI,GAMMA
      COMMON/BLOCKB/D50,SRATIO,NY,SLOPE,DFS
      COMMON/BLOCKC/CQ,CEQ,CEXO,EPS
      COMMON/BLOCKE/HBEG,ZBEG,T,DCHG,CC,DOFF
C*
      HO=HBEG
      DO 3 I=1,5
        NPP(I)=0
        NPE(I)=0
        NPB(I)=0
3      CONTINUE
      LO=1.5613*T**2
      J=0
      L=0
      DO 5 I=1,M-1
C*
C* DETERMINE LOCATION OF BREAK POINTS, PLUNGE POINTS AND
C* CORRESPONDING SPATIAL DECAY COEFFICIENTS
C*
        IF(NBR(I) .EQ. 1 .AND. NBR(I+1) .EQ. 0) THEN
          J=J+1
          NPB(J)=I
          CEXO(J)=0.40*(D50*1E3/H(I))**0.47
          NPP(J)=NPB(J)-NINT(3*H(I)/DX)
        ENDIF
C*
C* DETERMINE LOCATION OF REFORMATION POINTS
C*
        IF(NBR(I) .EQ. 0 .AND. NBR(I+1) .EQ. 1) THEN
          L=L+1
          NPE(L)=I+1
        ENDIF
5      CONTINUE
      NRBPE=J
C*
C* DETERMINE THE RUNUP LIMIT ACCORDING TO RELATIONSHIP FROM CE
C* AND CRIEPI DATA
C*
      DRU=-1.47*HO*(TAN(SLOPE)/SQRT(HO/LO))**0.79

```

```

C*
C* DETERMINE THE LOCATION OF THE SURF ZONE END AND RUNUP LIMIT.
C* WHEN A BOUNDARY DEPTH OCCUR IN THE MIDDLE OF A GRID CELL THE
C* THE SEAWARD BOUNDARY NUMBER OF THE CELL IS ASSIGNED TO THE
C* BOUNDARY INTEGER NUMBER
C*
      OK1=.TRUE.
      OK2=.TRUE.
      DO 9 I=M,1,-1
        IF((DH(I).LT.DRU.AND.DH(I+1).GE.DRU).AND.OK1)THEN
          NRU=I+1
          OK1=.FALSE.
        ENDIF
        IF((DHTOT(I).LT.DFS.AND.DHTOT(I+1).GE.DFS).AND.OK2)THEN
          NFS=I+1
          OK2=.FALSE.
        ENDIF
        IF((.NOT.OK1).AND.(.NOT.OK2)) GOTO 88
9      CONTINUE
      IF(OK1) NRU=1
88     DO 20 I=1,NRBPE
        IF(NPE(I).GT.NPP(I))THEN
          NPP(I)=NPE(I)
        ENDIF
20    CONTINUE
      RETURN
      END

```



```

C*
C*****
SUBROUTINE TRSIGN(SIGN)
C*****
C*
C* THIS ROUTINE DETERMINES THE DIRECTION OF THE SAND
C* TRANSPORT ALONG THE PROFILE. THE TRANSPORT IS DIRECTED
C* ONSHORE OR OFFSHORE DEPENDING ON THE VARIABLE SIGN
C* (SIGN = 1, OFFSHORE, = -1, ONSHORE) ACCORDING TO AN
C* EMPIRICAL EXPRESSION.
C*
      INTEGER SIGN
      REAL T,D50,LO,HO,VF,WSTP,DIMVF,SRATIO,B,NY,DCHG
      COMMON/BLOCKB/D50,SRATIO,NY,SLOPE,DFS
      COMMON/BLOCKC/HBEG,ZBEG,T,DCHG,CC,DOFF
      HO=HBEG
      LO=1.5613*T**2
      WSTP=HO/LO/1.6
C*
C* DETERMINE THE FALL VELOCITY ACCORDING TO HALLERMEIER
C*
      B=(SRATIO-1)*9.81*D50**3/NY**2
      IF(B.LE.39)THEN
        VF=(SRATIO-1)*9.81*D50**2/18/NY
      ELSEIF(B.GT.39.AND.B.LE.1E4)THEN
        VF=((SRATIO-1)*9.81)**0.7*D50**1.1/6/NY**0.4
      ELSE
        VF=((SRATIO-1)*9.81*D50/0.91)**0.5
      ENDIF
      DIMVF=HO/T/VF/1.6
C*
C* USE EMPIRICALLY DERIVED CRITERIA TO PREDICT TRANSPORT DIRECTION
C*
      IF(WSTP.LT.7E-4*DIMVF**3)THEN
        SIGN=1
      ELSE
        SIGN=-1
      ENDIF
      RETURN
      END

```

```

C*
C*****
SUBROUTINE XTRANS(SIGN,DMEAN,NRU,NFS,NPE,NPP,NPB,NRBPE,DISS,Q)
C*****
C*
C* THIS ROUTINE GENERATES THE CROSS-SHORE TRANSPORT RATES.
C*
      INTEGER I,NFS,NPP(5),NPE(5),NZ,MM,NN,NRU,M,SIGN,NPB(5),
&NRBPE,N
      PARAMETER(MM=100,NN=50,NNGR=10,NM=NN*MM,
&M1=MM+1,N1=NN+1,NM1=M1*N1)
      REAL DX,DTX,DMEAN(MM),Q(M1),QSMO(M1),DISS(MM),CEXO(5),DY,
&CQ,CEQ,EPS,CRED,CEXR,AEXP,CEXP
      LOGICAL END,REDUCE
C*
      COMMON/BLOCKA/DX,DY,DTX,M,N,G,PI,GAMMA
      COMMON/BLOCKC/CQ,CEQ,CEXO,EPS
      COMMON/BLOCKD/CRED,CEXR,AEXP
C*
C* DETERMINE THE Q-VALUES ON THE NEXT TIME LEVEL
C*
      END=.FALSE.
      IF(NPE(1).LT.NFS) NPE(1)=NFS
      IF(NPP(1).LT.NFS) NPP(1)=NFS
C*
C* DETERMINE TRANSPORT RATES IN AREAS OF BROKEN WAVES
C*
      DO 5 I=1,NRBPE
        REDUCE=.FALSE.
C*
C* IF THE BROKEN WAVE ZONE IS ONLY ONE CELL WIDE REDUCE THE
C* TRANSPORT
C*
        IF(I.EQ.1.AND.NPP(I)-NPE(I).LE.1) REDUCE=.TRUE.
77      DO 10 J=NPE(I),NPP(I)
          IF(J.NE.NPE(I))THEN
            Q(J)=REAL(SIGN)*CQ*(0.5*(DISS(J)+DISS(J-1))-CEQ)+
& EPS*(DMEAN(J)-DMEAN(J-1))/DX
            IF(REAL(SIGN)*Q(J).LT.0)THEN
              Q(J)=0
            ENDIF
          ELSE
            IF(I.EQ.1)THEN
              Q(J)=REAL(SIGN)*CQ*(DISS(J)-CEQ)+
& EPS*(DMEAN(J+1)-DMEAN(J))/DX
              IF(REAL(SIGN)*Q(J).LT.0)THEN
                Q(J)=0
              ENDIF
            ENDIF
C*
C* REDUCTION OF TRANSPORT RATE FOR NARROW SURF ZONE
C*
            IF(REDUCE) Q(J)=Q(J)*CRED
          ELSE
            Q(J)=REAL(SIGN)*CQ*(DISS(J)-CEQ)+
& EPS*(DMEAN(J)-DMEAN(J-1))/DX
            IF(REAL(SIGN)*Q(J).LT.0)THEN

```

```

                                Q(J)=0
                                ENDIF
                                ENDIF
                                ENDIF
10      CONTINUE
5      CONTINUE
      DO 25 I=1,NRBPE
        IF(I.EQ.NRBPE) END=.TRUE.
        CEXP=CEXO(I)/5.
C*
C* DETERMINE TRANSPORT RATES SEAWARD OF FIRST BREAK POINT
C*
        IF(END)THEN
C*
C* ... FROM PLUNGE POINT TO BREAK POINT
C*
          DO 11 J=NPP(I)+1,NPB(I)
            Q(J)=Q(NPP(I))*EXP(-CEXP*DX*REAL(J-NPP(I)))
11      CONTINUE
C*
C* ... FROM BREAK POINT TO END OF GRID
C*
          DO 12 J=NPB(I)+1,M
            Q(J)=Q(NPB(I))*EXP(-CEXO(I)*DX*REAL(J-NPB(I)))
            IF(ABS(Q(J)).LT.ABS(Q(NPB(I)))/100.)THEN
              NZ=J
              GOTO 66
            ENDIF
12      CONTINUE
          ELSE
C*
C* DETERMINE TRANSPORT RATES BETWEEN ZONES OF BROKEN WAVES SHOREWARD
C* OF THE FIRST BREAK POINT
C* ...FROM PLUNGE POINT TO BREAK POINT
C*
          DO 15 J=NPP(I)+1,NPB(I)
            Q(J)=Q(NPP(I))*EXP(-CEXP*DX*REAL(J-NPP(I)))
15      CONTINUE
C*
C* ...FROM BREAK POINT TO REFORMATION POINT
C*
          NMP=NPB(I)+(NPE(I+1)-NPB(I))/3
          C      WRITE(*,*) NPP(I),NPB(I),NPE(I+1),NMP
          C      WRITE(*,*) Q(NPP(I)),Q(NPB(I)),Q(NPE(I+1))
          DO 20 J=NPE(I+1)-1,NMP,-1
            Q(J)=Q(NPE(I+1))*EXP(-CEXR*DX*REAL(NPE(I+1)-J))
20      CONTINUE
          DO 30 J=NPB(I)+1,NMP-1
            Q(J)=(Q(NPB(I))-Q(NMP))*(1-(REAL(J-NPB(I))/
          & REAL(NMP-NPB(I)))*AEXP)+Q(NMP)
30      CONTINUE
          ENDIF
66      END=.FALSE.
25      CONTINUE
      IF(NPE(1).NE.NFS)THEN
        DO 40 J=NPE(1)-1,NFS,-1

```

```

      Q(J)=Q(NPE(1))*EXP(-CEXR*DX*REAL(NPE(1)-J))
40      CONTINUE
      ENDIF
C*
C* DETERMINE TRANSPORT RATES IN THE SWASH ZONE
C*
      DO 50 J=NRU+1,NFS-1
          Q(J)=Q(NFS)*(REAL(J)-REAL(NRU))/REAL(NFS-NRU)
50      CONTINUE
C*
C* DETERMINE TRANSPORT RATES AT THE BOUNDARIES
C*
      Q(NRU)=0
      Q(NZ+1)=0
C*
C* ZERO Q-ARRAY OUTSIDE TRANSPORT REGIONS
C*
      DO 80 I=1,NRU-1
          Q(I)=0
80      CONTINUE
      DO 90 I=NZ+2,M
          Q(I)=0
90      CONTINUE
      RETURN
      END

```

```

C*
C*****
      SUBROUTINE BATHYM(QX,QY,D)
C*****
C*
C* THIS ROUTINE CALCULATES THE CHANGES IN BATHYMETRY FROM
C* THE MASS CONSERVATION EQUATION. THE TRANSPORT RATE MUST
C* BE GENERATED WHEN THIS SUBROUTINE IS CALLED
C*
      INTEGER MM,NN,I,J,M,N
      PARAMETER(MM=100,NN=50,NNGR=10,NM=NN*MM,
&M1=MM+1,N1=NN+1,NM1=M1*N1)
      REAL QX(M1,N1),D(MM,NN),DX,DY,DTX,QY(M1,N1)
      INTEGER ISHORE(NN)

C*
      COMMON/BLOCKA/DX,DY,DTX,M,N,G,PI,GAMMA

C*
      DO 10 J=1,N
        DO 20 I=1,M

C*
C* CALCULATE THE NEW DEPTHS ALONG THE GRID
C*
          D(I,J)=D(I,J)+DTX/DX*(QX(I+1,J)-QX(I,J))+
&      DTX/DY*(QY(I,J+1)-QY(I,J))
20      CONTINUE
          CALL MAXANG(J,D,2,M,ISHORE(J))
10      CONTINUE
      RETURN
      END

```

```

C*
C*****
      SUBROUTINE MAXANG(IP,D,NBEG,NEND,ISHOR)
C*****
C*
C* THIS ROUTINE LIMITS THE STEEPNESS OF THE PROFILE BY INITIATING
C* AVALANCHING WHEN THE SLOPE LOCALLY EXCEEDS A PREDEFINED
C* MAXIMUM VALUE. THE AVALANCHING IS CONSIDERED TO OCCUR INFINITELY
C* FAST IN COMPARISON WITH THE TIME STEP OF THE MODEL. SAND IS
C* REDISTRIBUTED IN THE NEIGHBORING CELLS AT A SLOPE CORRESPONDING
C* TO THE STABLE SLOPE AFTER AVALANCHING.
C*
      INTEGER NBEG,NEND,MM,NN,I,NCORR,NDIR,NVAL,J,L,IMAX,IP,ISHOR,
&M,N
      PARAMETER(MM=100,NN=50,NNGR=10,NM=NN*MM,
&M1=MM+1,N1=NN+1,NM1=M1*N1)
      REAL D(MM,NN),DD(MM),BMAX,BAV,DX,DTX,BPMAX,DCORR,DCR,DSUM,
&DDCRIT,DY
      LOGICAL CHECK
C*
      COMMON/BLOCKA/DX,DY,DTX,M,N,G,PI,GAMMA
C*
      BAV=0.3
      BMAX=0.5
      L=0
C*
C* DETERMINE THE MAXIMUM SLOPE ALONG THE PROFILE
C*
88      CHECK=.FALSE.
          L=L+1
          BPMAX=0
          DO 10 I=NBEG,NEND-1
              IF(ABS((D(I,IP)-D(I-1,IP))/DX).GT.ABS(BPMAX))THEN
                  BPMAX=(D(I,IP)-D(I-1,IP))/DX
                  IMAX=I
              ENDIF
C*
C* DETERMINE THE LOCATION OF THE SHORELINE FOR PROFILE IP
C*
          IF(D(I-1,IP).LE.0.AND.D(I,IP).GT.0) ISHOR=I-1
10      CONTINUE
C*
C* CHECK IF THE MAXIMUM SLOPE EXCEEDS THE ANGLE OF REPOSE
C*
          IF(ATAN(ABS(BPMAX)).GT.BMAX) CHECK=.TRUE.
          IF(CHECK)THEN
              WRITE(*,*) '/ AVALANCHIIIIII.....'
C*
C* REDISTRIBUTE THE SAND IN THE NEIGHBORING CELLS ACCORDING TO THE
C* SLOPE AFTER AVALANCHING HAS OCCURRED (BAV)
C*
              DCR=DX*TAN(BAV)
              IF(BPMAX.GT.0)THEN
                  NDIR=-1
              ELSE
                  NDIR=1

```

```

      IMAX=IMAX-1
      ENDIF
      NCORR=IMAX
77      NCORR=NCORR+NDIR
C*
C* CONTINUE TO REDISTRIBUTE SAND UNTIL THE FIRST CELL OUTSIDE THE AREA
C* WHERE SAND IS MOVED HAS A SLOPE LOWER THAN BAV
C*
      NVAL=1
      DSUM=0
      DO 20 I=IMAX+NDIR,NCORR,NDIR
        IF(I.GT.NEND.OR.I.LT.NBEG-1)THEN
          WRITE(*,*) 'AV STOP',I,IMAX+NDIR,NCORR,L
          STOP
        ENDIF
        DSUM=DSUM+D(I,IP)
        NVAL=NVAL+1
20      CONTINUE
      DCORR=-D(IMAX,IP)*(NVAL-1)/NVAL+DSUM/NVAL+DCR/2*(NVAL-1)
      DD(IMAX)=D(IMAX,IP)+DCORR
      J=1
C*
C* CALCULATE THE NEW DEPTHS
C*
      DO 30 I=IMAX+NDIR,NCORR,NDIR
        J=J+1
        DCORR=DD(IMAX)-D(I,IP)-REAL(J-1)*DCR
        DD(I)=D(I,IP)+DCORR
30      CONTINUE
      IF(NCORR+NDIR.GE.NBEG-1)THEN
        IF(NDIR.EQ.-1)THEN
          DDCRIT=(DD(NCORR)-D(NCORR+NDIR,IP))/DX
          IF(DDCRIT.GT.TAN(BAV)) GOTO 77
        ELSE
          DDCRIT=(D(NCORR+NDIR,IP)-DD(NCORR))/DX
          IF(DDCRIT.LT.-TAN(BAV)) GOTO 77
        ENDIF
      ENDIF
      DO 40 I=IMAX,NCORR,NDIR
        D(I,IP)=DD(I)
40      CONTINUE
      ENDIF
C*
C* GO BACK AND CHECK IF THE ANGLE OF REPOSE IS EXCEEDED IN OTHER
C* PARTS OF THE PROFILE
C*
      IF(CHECK.AND.L.LT.20) GOTO 88
      IF(L.GE.20) WRITE(*,*) 'AVALANCHING ROUTINE NOT CONVERGING'
      IF(L.GE.20) STOP
      RETURN
      END

```

```

C*
C*****
SUBROUTINE CONPLA(D,JP,DMEAN,ZC,ZCM)
C*****
C*
C* THIS ROUTINE CALCULATES THE AVERAGE PROFILE DEPTH BETWEEN
C* TWO NEIGHBORING LINES. ALSO, THE CONTOUR ORIENTATION IS
C* DETERMINED USING AN AVERAGE OF TWO PLANES FITTED THROUGH
C* THREE POINTS AROUND THE CALCULATION POINT.
C*
PARAMETER (MM=100,NN=50,NNGR=10,NM=NN*MM,
&M1=MM+1,N1=NN+1,NM1=M1*N1)
INTEGER JL,JR,JP,KK
REAL D(MM,NN),DMEAN(M1),ZC(MM),ZCM
COMMON/BLOCKA/DX,DY,DTX,M,N,G,PI,GAMMA
C*
C* CALCULATE MEAN WATER DEPTH
C*
IF(JP.EQ.1)THEN
DO 10 I=1,M
DMEAN(I)=D(I,1)
10 CONTINUE
JL=1
JR=2
ELSEIF(JP.EQ.N+1)THEN
DO 20 I=1,M
DMEAN(I)=D(I,N)
20 CONTINUE
JL=N-1
JR=N
ELSE
DO 30 I=1,M
DMEAN(I)=0.5*(D(I,JP)+D(I,JP-1))
30 CONTINUE
JL=JP-1
JR=JP
ENDIF
C*
C* DETERMINE CONTOUR ORIENTATION
C*
DO 40 I=2,M-1
IF(D(I+1,JL)-D(I-1,JL).GT.0.001)THEN
BSC1=DX*(2*D(I,JR)-D(I-1,JL)-D(I+1,JL))/DY/(D(I+1,JL)
& -D(I-1,JL))
ELSE
BSC1=1000.
ENDIF
Z1=ATAN(-BSC1)
IF(D(I+1,JR)-D(I-1,JR).GT.0.001)THEN
BSC2=DX*(D(I-1,JR)+D(I+1,JR)-2*D(I,JL))/DY/(D(I+1,JR)
& -D(I-1,JR))
ELSE
BSC2=1000.
ENDIF
Z2=ATAN(-BSC2)
ZC(I)=0.5*(Z1+Z2)

```



```

40    CONTINUE
      ZC(1)=ZC(2)
      ZC(M)=ZC(M-1)
C*
C* DETERMINE AVERAGE CONTOUR ORIENTATION FOR A PROFILE LINE
C*
      KK=0
      ZCM=0.0
      DO 50 I=M-1,1,-1
        IF(D(I,JP).LT.0) GOTO 99
        ZCM=ZCM+ZC(I)
        KK=KK+1
50    CONTINUE
99    ZCM=ZCM/REAL(KK)
      IF(ABS(ZCM).LT.1.0E-6) ZCM=0.0
      RETURN
      END

```

```

C*
C*****
      SUBROUTINE WAVEHD(KKK,D,J,H,E,V,DISS,ISTOP,NBR,
&ZC,ZCM)
C*****
C*
C* THIS ROUTINE DETERMINES THE WAVE HEIGHT DISTRIBUTION
C* ACROSS-SHORE FOR A SPECIFIC PROFILE J.
C*
      INTEGER MM,NN,NNGR,NM,M1,N1,NM1,J,I
      PARAMETER (MM=100,NN=50,NNGR=10,NM=NN*MM,M1=MM+1,
&N1=NN+1,NM1=M1*N1)
      INTEGER NBR(M1),M,ISTOP
      REAL D(MM,NN),DHTOT(M1),H(M1),ZW(M1),SXX(M1),V(M1),
&SXY(M1),DMEAN(MM),DH(M1),DSEND,CC,PI,ZC(MM),ZCC(MM),
&HBEG,ZBEG,T,L1,CG1,CN1,E(M1),F(M1),L2,CG2,CN2,ZTEMP1,
&ZTEMP2,GAMMA,KAPPA,AC,FSTAB,DISS(MM),DFS,ZCM,DCHG,LO
      LOGICAL BREAK
      COMMON/BLOCKA/DX,DY,DTX,M,N,G,PI,GAMMA
      COMMON/BLOCKB/D50,SRATIO,NY,SLOPE,DFS
      COMMON/BLOCKC/HBEG,ZBEG,T,DCHG,CC,DOFF
      DATA KAPPA/0.15/
      BREAK=.FALSE.
      DSEND=0.4*DFS
C*
C* ZERO ARRAY CONTAINING INFORMATION ABOUT BROKEN WAVES
C*
      DO 3 I=1,M+1
          NBR(I)=0
          E(I)=0
      3   CONTINUE
C*
C* DETERMINE AVERAGE DEPTH BETWEEN NEIGHBORING PROFILES
C* AND THE LOCAL CONTOUR ORIENTATION
C*
      CALL CONPLA(D,J,DMEAN,ZCC,ZCM)
      DO 2 I=2,M
          DH(I)=(DMEAN(I-1)+DMEAN(I))/2.
      2   CONTINUE
      DH(M+1)=DMEAN(M)
      DH(1)=DMEAN(1)
C*
C* CONVERT LOCAL COUNTER ANGLE TO REFERENCE SYSTEM WITH RESPECT
C* TO THE X-AXIS POINTING OFFSHORE
C*
      DO 5 I=1,M
          ZC(I)=PI/2.-ZCC(I)
      5   CONTINUE
      ZCM=PI/2.-ZCM
C*
C* DETERMINE WAVE PROPERTIES IN THE MOST SEAWARD CALCULATION CELL
C* WHEN THE DEEPWATER WAVE CONDITIONS ARE GIVEN
C*
      IF(DOFF.LT.0)THEN
          LO=1.5613*T**2
          FOFF=CC*HBEG**2*LO/T/2

```

```

ELSE
  CALL LINWAV(T,DOFF,LO,CGO,CNO)
  FOFF=CC*HBEG**2*CGO
ENDIF
CALL LINWAV(T,DH(M+1),L1,CG1,CN1)
ZTEMPO=ZBEG-ZCM
ZTEMP1=ASIN(L1/LO*SIN(ZTEMPO))
ZW(M+1)=ZTEMP1+ZCM
F(M+1)=FOFF*COS(ZTEMPO)/COS(ZTEMP1)
H(M+1)=SQRT(F(M+1)/GC/CG1)
E(M+1)=-PI*H(M+1)**2/4./L1/SINH(4*PI*DH(M+1)/L1)
SXX(M+1)=CC*H(M+1)**2*(CN1*((COS(ZW(M+1)-ZCM))**2+1)-0.5)
SXY(M+1)=0.5*CC*HBEG**2*CN1*SIN(2*(ZW(M+1)-ZCM))
C*
C* PROCEED FROM THE END OF THE GRID IN THE SHOREWARD DIRECTION
C* WHEN CALCULATING WAVE PROPERTIES ACROSS-SHORE
C*
  DO 10 I=M,1,-1
C*
C* DETERMINE WAVE PROPERTIES FROM LINEAR WAVE THEORY
C*
  ETEST=E(I+1)
  IF(DH(I).LT.0) ETEST=E(I+1)+E(I+1)-E(I+2)
  IF(DH(I)+ETEST.LT.0)THEN
    ISTOP=I+1
    GOTO 77
  ENDIF
  CALL LINWAV(T,DH(I)+ETEST,L2,CG2,CN2)
C*
C* CALCULATE WAVE REFRACTION FROM SNELLS LAW USING THE LOCAL
C* CONTOUR ORIENTATION
C*
  ZTEMP1=ZW(I+1)-ZCM
  ZTEMP2=ASIN(L2/L1*SIN(ZTEMP1))
  ZW(I)=ZTEMP2+ZCM
C*
C* APPLY DALLY'S BREAKER DECAY MODEL USING THE ENERGY FLUX
C*
88  IF(H(I+1).GT.GAMMA*(DH(I+1)+E(I+1)).OR.BREAK)THEN
    EMEAN=0.5*(ETEST+E(I+1))
    AC=KAPPA*DX/(DMEAN(I)+EMEAN)
    FSTAB=CC*(0.4*(DMEAN(I)+EMEAN))**2*(CG1+CG2)/2.
    BREAK=.TRUE.
    NBR(I+1)=1
  C    WRITE(*,*) 'WAVE ',I,' IS BROKEN'
  ELSE
    AC=0
    FSTAB=0.0
    NBR(I+1)=0
    DISS(I)=0
  C    WRITE(*,*) 'WAVE ',I,' IS NOT BROKEN'
  ENDIF

```

```

C*
C* CALCULATE THE ENERGY FLUX
C*
      F(I)=(F(I+1)*(COS(ZTEMP1)-0.5*AC)+AC*FSTAB)/(COS(ZTEMP2)
& +0.5*AC)
      IF(F(I).LT.0)THEN
        ISTOP=I+1
        GOTO 77
      ENDIF
C*
C* CALCULATE THE ENERGY DISSIPATION PER UNIT VOLUME IN REGIONS OF
C* BROKEN WAVES
C*
      IF(BREAK) DISS(I)=KAPPA/(DMEAN(I)+E(I+1))**2*((F(I)+
& F(I+1))/2.-FSTAB)
C*
C* CHECK IF THE WAVE IS REFORMING BEFORE REACHING GRID POINT I
C*
      IF((F(I)+F(I+1))/2..LT.FSTAB)THEN
        BREAK=.FALSE.
        DISS(I)=0
        WRITE(*,*) 'SHOALING - HERE WE GO AGAIN'
        GOTO 88
      ENDIF
C*
C* CALCULATE THE WAVE HEIGHT FROM THE ENERGY FLUX
C*
      H(I)=SQRT(F(I)/CC/CG2)
C*
C* CALCULATE THE RADIATION STRESSES SXX AND SKY
C*
      SXX(I)=CC*H(I)**2*(CN2*(COS(ZTEMP2))**2+1)-0.5)
      SKY(I)=0.5*CC*H(I)**2*CN2*SIN(2*ZTEMP2)
C*
C* CALCULATE THE WAVE SET-DOWN OR SET-UP
C*
      E(I)=E(I+1)+(SXX(I+1)-SXX(I))/8./CC/(DMEAN(I)+E(I+1))
      IF(DH(I)+E(I).LT.0)THEN
        ISTOP=I+1
        GOTO 77
      ENDIF
C*
C* UPDATE WAVE PARAMETERS
C*
      CN1=CN2
      CG1=CG2
      L1=L2
C      IF(I.GT.1.AND.DH(I-1).LT.0) GOTO 99
      IF(DH(I)+E(I).LT.DSEND) GOTO 99
10    CONTINUE
C*
C* CALCULATE THE TOTAL DEPTH
C*
99    IF(H(I).GT.GAMMA*(DH(I)+E(I))) NBR(I)=1
      IF(NBR(I+1).EQ.1.AND.0.5*(F(I)+F(I+1))-FSTAB.GT.0) NBR(I)=1
      IF(I.GT.0)THEN

```

```

      ISTOP=I
    ELSE
      ISTOP=1
    ENDIF
77  DO 20 I=ISTOP,M+1
      DHTOT(I)=DH(I)+E(I)
20  CONTINUE
C*
C* WRITE RESULT TO FILE
C*
    IF(J.LE.5.AND.KKK.EQ.1)THEN
      WRITE(24,300) 'NR','D','DMEAN','DM','ZC','ZCC','ZW'
300  FORMAT(' ',TR2,A,TR4,A,TR4,A,TR5,A,TR6,A,TR5,A,TR6,A)
      WRITE(24,*)
      WRITE(21,400) 'NR','H','E','SXX','SXY','DISS','ZCM'
400  FORMAT(' ',TR2,A,TR4,A,TR5,A,TR5,A,TR4,A,TR4,A,TR4,A)
      WRITE(21,*)
    C    WRITE(22,*) M-ISTOP+1
      CRD=180./PI
      DO 30 I=ISTOP,M
        Z1=90.-ZC(I)*CRD
        Z2=90.-ZCC(I)*CRD
        Z3=90.-ZW(I)*CRD
        WRITE(24,100) I,D(I,J),DMEAN(I),DH(I),Z1,Z2,Z3
        WRITE(21,200) I,H(I),E(I),SXX(I),SXY(I),DISS(I),ZCM
100    FORMAT(' ',I3,3F8.3,3F8.1)
200    FORMAT(' ',I3,2F8.3,3F8.1,F8.3)
    C    WRITE(22,*) REAL(I),H(I)
30  CONTINUE
      ENDIF
    C    WRITE(22,*) M-ISTOP+1
      DO 40 I=ISTOP,M
    C    WRITE(22,*) REAL(I),-DH(I)
40  CONTINUE
C*
C* DETERMINE THE LONGSHORE CURRENT
C*
      CALL VELOC(ISTOP,NBR,H,ZW,ZC,ZCM,SXY,DHTOT,V)
      RETURN
      END

```

```

C*
C*****
SUBROUTINE LINWAV(T,DD,L,CG,CN)
C*****
C*
C* THIS ROUTINE CALCULATES THE WAVE LENGTH, GROUP VELOCITY,
C* AND THE CONSTNANT N AT A SPECIFIED DEPTH D
C*
      INTEGER M,N
      REAL T,DD,L,CG,CN,PI,G,DX,DY,DTX
      COMMON/BLOCKA/DX,DY,DTX,M,N,G,PI,GAMMA
C*
C* USE A PADE APPROXIMATION TO CALCULATE THE WAVE LENGTH
C*
      Y=(2*PI/T)**2*DD/G
      F=Y+1./(1.+Y*(0.66667+Y*(0.3555+Y*(0.16084+Y*(0.06320+
&Y*(0.02174+Y*(0.00654+Y*(0.00171+Y*(0.00039+Y*0.000111
&)))))))))
      L=2*PI/SQRT(Y*F/DD**2)
      C=4*PI*DD/L
      CN=0.5*(1+C/SINH(C))
      CG=CN*L/T
      RETURN
      END

```

```

C*
C*****
      SUBROUTINE VELOC(IS,NBR,H,ZW,ZC,ZCM,SXY,DHTOT,V)
C*****
C*
C* CALCULATES LONGSHORE CURRENT DISTRIBUTION OVER AN ARBITRARY
C* BOTTOM PROFILE; WATER DEPTH & WAVE INFORMATION GIVEN EXTERNALLY
C*
      INTEGER I,IS,MM,NN,NNGR,NM,M1,N1,NM1,M,N
      PARAMETER(MM=100,NN=50,NNGR=10,NM=NN*MM,
&M1=MM+1,N1=NN+1,NM1=M1*N1)
      INTEGER NBR(M1)
      REAL H(M1),ZW(M1),DHTOT(M1),V(M1),UM(M1),EPS(M1),EE(MM),
&FF(MM),DX,DTX,G,PI,AI,AHAT,BHAT,CHAT,RHAT,DEN,ZCM,DCHG,
&GAMMIX,CF,ALPHA,L,CG,CN,ZC(MM),HBEG,ZBEG,T,SXY(M1),KY
      COMMON/BLOCKA/DX,DY,DTX,M,N,G,PI,GAMMA
      COMMON/BLOCKE/HBEG,ZBEG,T,DCHG,CC,DOFF
      COMMON/BLOCKF/CF,GAMMIX,KY,QCUT
      ALPHA=0.0
      DXSQ=DX**2
C*
C* BOTTOM ORBITAL VELOCITY
C*
      DO 10 I = IS,M+1
          CALL LINWAV(T,DHTOT(I),L,CG,CN)
          UM(I)=0.5*H(I)*G*T/L/COSH(2*PI*DHTOT(I)/L)
          EPS(I)=GAMMIX*UM(I)*H(I)
          SXY(I)=SXY(I)/1000.
10      CONTINUE
C*
C* SOLVE FOR VELOCITY
C* -----
C* BOUNDARY CONDITION FOR VELOCITY ON SHOREWARD SIDE < V(IS+1) >
C* NOTE X_AXIS SHOULD POINT ONSHORE FOR DFN OF STRESSES
C*
      ZI = 0.5*( ZW(IS+1) + ZW(IS)) -ZCM
      UMI=0.5*(UM(IS+1)+UM(IS))
      V(IS) = -(SXY(IS+1) - SXY(IS))/DX
& /((2./PI*UMI*CF*(1 + SIN(ZI)**2))
      EE(IS) = 0.0
      FF(IS) = V(IS)
C*
C* FORWARD SWEEP
C*
      AI=EPS(IS+1)*DHTOT(IS+1)
      DO 11 I = IS+1, M
          IN=I+1
          IP=I-1
          UMI=0.5*(UM(IN)+UM(I))
          AIN=EPS(IN)*DHTOT(IN)
          AHAT = -AI/DXSQ
          CHAT = -AIN/DXSQ
          ZI = 0.5*(ZW(IN) + ZW(I)) -ZCM
          BI = 2./PI*CF*UMI*(1. + SIN(ZI)**2)
          BHAT = -(BI + (AI+AIN)/DXSQ)
          RHAT = (SXY(IN) - SXY(I))/DX + ALPHA

```

```

DEN = BHAT - AHAT*EE(IP)
EE(I) = CHAT/DEN
FF(I) = (AHAT*FF(IP) + RHAT)/DEN
AI=AIN
11  CONTINUE
C*
C*  BOUNDARY CONDITION FOR VELOCITY AT SEAWARD SIDE < V(M1) >
C*
      V(M+1) = 0.0
C*
C*  BACKWARD SWEEP
C*
      DO 21 I = M, IS+1, -1
        V(I) = EE(I)*V(I+1) + FF(I)
21  CONTINUE
      IVS=IVS+1
C*
C*  -----  END OF V CALCULATION
C*
C      DO 55 I=IS,M
C        WRITE(23,100) I, EPS(I), H(I), H(I+1), UM(I), V(I)
C100      FORMAT(' ', I3, TR2, F8.5, 5(TR2, F8.3))
C55  CONTINUE
C      WRITE(23,*)
C      WRITE(23,*)
      RETURN
      END

```



```

C*
C*****
      SUBROUTINE TRANY(IP,ISTOP,NRU,NFS,NBR,V,H,ZC,ZCM,QY,
&QYX)
C*****
C*
C* THIS ROUTINE DETERMINES THE LONGSHORE TRANSPORT RATE ACROSS
C* THE SURF ZONE ACCORDING TO THE KRAUS FORMULA.
C*
      PARAMETER(MM=100,NN=50,NNGR=10,NM=NN*MM,
&M1=MM+1,N1=NN+1,NM1=M1*N1)
      INTEGER ISTOP,M,N,NBR(M1),IBRIGH,IBLEFT
      REAL V(M1),H(M1),QY(M1,N1),DX,DY,DTX,G,PI,KY,ZC(MM),
&QYX(M1,N1)
      COMMON /BLOCKA/DX,DY,DTX,M,N,G,PI,GAMMA
      COMMON /BLOCKF/CF,GAMMIX,KY,QCUT
      COMMON /BLOCKG/IBRIGH,IBLEFT
C*
C* DETERMINE LONGSHORE TRANSPORT RATE
C*
      IF(IP.GT.1.AND.IP.LT.N+1)THEN
        DO 5 I=1,ISTOP-1
          QY(I,IP)=0
5        CONTINUE
        IF(ISTOP.GT.NFS)THEN
          WRITE(*,*) 'TOO BAD - NFS < ISTOP'
        ENDIF
        DO 10 I=ISTOP,M
          DO 10 I=NFS+5,M
            HAV=0.5*(H(I)+H(I+1))
            QY(I,IP)=KY*V(I)*HAV-QCUT
10        CONTINUE
        DO 33 I=NRU,NFS+4
          QY(I,IP)=QY(NFS+5,IP)
C        CONTINUE
C33      ELSEIF(IP.EQ.1)THEN
C*
C* SET BOUNDARY CONDITION AT RIGHT END OF GRID
C*
        DO 15 I=1,M
          IF(IBRIGH.EQ.1) QY(I,1)=0
15        CONTINUE
        ELSE
C*
C* SET BOUNDARY CONDITION AT LEFT END OF GRID
C*
        DO 25 I=1,M
          IF(IBLEFT.EQ.1)THEN
            QY(I,N+1)=0
          ELSE
            QY(I,N+1)=QY(I,N)
            QYX(I,N+1)=QYX(I,N)
          ENDIF
25        CONTINUE
      ENDIF
C*

```

```

C* MODIFY TRANSPORT RATE ACCORDING TO LOCAL CONTOUR
C*
      IF(IBLEFT.NE.0.OR.IP.NE.N+1)THEN
        DO 35 I=1,M
          QY(I,IP)=QY(I,IP)*COS(PI/2.-ZCM)
          QYX(I,IP)=QY(I,IP)*SIN(PI/2.-ZCM)
35      CONTINUE
        ENDIF
        QYX(M+1,IP)=0.0
        RETURN
      END

```

APPENDIX B

HEADING
HEADING
HEADING
HEADING
RUN TITLE:
2D-TEST RUN
B. NUMBER OF CALCULATION LOOPS AND CELLS: NCL, M(C-S), N(L-S)
160 100 10
F. TIME AND SPACE INTERVAL: DT(MIN), DX(M), DY(M)
20 2 20
LONGSHORE TRANSPORT PARAMETERS: CF,GAMMIX
0.01 1.0
MEDIAN SAND GRAIN SIZE: D50(MM)
0.2
OUTPUT INTERVAL EXPRESSED AS NO. OF CALC. TIME LOOPS: IOUT
160
N. DEPTH CORRESPONDING TO OFFSHORE WAVE DATA: DZ
2.96
U. SAND TRANSPORT CALIBRATION COEFFICIENTS: KY(L-S), KX(C-S)
5E-4 0.5
BOUNDARY CONDITIONS (0=OPEN COAST, 1=GROIN)
1 0